



Evaluating methodologies for species delimitation: the mismatch between phenotypes and genotypes in lichenized fungi (*Bryoria* sect. *Implexae*, *Parmeliaceae*)

C.G. Boluda^{1,2}, V.J. Rico¹, P.K. Divakar¹, O. Nadyeina², L. Myllys³, R.T. McMullin⁴, J.C. Zamora^{1,5}, C. Scheidegger², D.L. Hawksworth⁶

Key words

chemotypes
cryptic species
haplotypes
incomplete lineage sorting
integrative taxonomy
microsatellites
speciation
species concepts

Abstract In many lichen-forming fungi, molecular phylogenetic analyses lead to the discovery of cryptic species within traditional morphospecies. However, in some cases, molecular sequence data also questions the separation of phenotypically characterised species. Here we apply an integrative taxonomy approach – including morphological, chemical, molecular, and distributional characters – to re-assess species boundaries in a traditionally speciose group of hair lichens, *Bryoria* sect. *Implexae*. We sampled multilocus sequence and microsatellite data from 142 specimens from a broad intercontinental distribution. Molecular data included DNA sequences of the standard fungal markers ITS, IGS, *GAPDH*, two newly tested loci (FRBi15 and FRBi16), and SSR frequencies from 18 microsatellite markers. Datasets were analysed with Bayesian and maximum likelihood phylogenetic reconstruction, phenogram reconstruction, STRUCTURE Bayesian clustering, principal coordinate analysis, haplotype network, and several different species delimitation analyses (ABGD, PTP, GMYC, and DISSECT). Additionally, past population demography and divergence times are estimated. The different approaches to species recognition do not support the monophyly of the 11 currently accepted morphospecies, and rather suggest the reduction of these to four phylogenetic species. Moreover, three of these are relatively recent in origin and cryptic, including phenotypically and chemically variable specimens. Issues regarding the integration of an evolutionary perspective into taxonomic conclusions in species complexes, which have undergone recent diversification, are discussed. The four accepted species, all epitypified by sequenced material, are *Bryoria fuscescens*, *B. glabra*, *B. kockiana*, and *B. pseudofuscescens*. Ten species rank names are reduced to synonymy. In the absence of molecular data, they can be recorded as the *B. fuscescens* complex. Intraspecific phenotype plasticity and factors affecting the speciation of different morphospecies in this group of *Bryoria* are outlined.

Article info Received: 21 December 2017; Accepted: 18 June 2018; Published: 23 August 2018.

INTRODUCTION

Accurate identification and characterization of species is the basis of communication, conservation, resources management, and material used in biological research. However, in groups of relatively recent origin, species delimitation is often difficult (Jakob & Blattner 2006, Leavitt et al. 2011, Lumley & Sperling 2011). Organisms are always evolving, changing in response to either selective pressures or genetic drift, so that delimiting units to accord species names is not always clear (Naciri & Linder 2015). Several phenomena can hinder species delimitation: phylogenetic/phenotypic mismatches (Articus et al. 2002, Mark et al. 2016, Pino-Bodas et al. 2016), ‘intermediate’ specimens between generally accepted taxa (Seymour et al. 2007), hybridization (Konrad et al. 2002, Steinová et al. 2013), an absence

of delimited clades (Jakob & Blattner 2006, Lumley & Sperling 2011), or incomplete lineage sorting (Saag et al. 2014, Leavitt et al. 2016). Long-term reproductive isolation may produce structured, non-overlapping lineages, whereas an intraspecific phylogeny, as well as a recent or contemporary speciation event, may produce reticulated lineages (Abbott et al. 2016).

The family *Parmeliaceae* is one of the most studied amongst lichenised fungi. It contains many genera with species delimitation problems, such as *Cetraria aculeata* (Lutsak et al. 2017); *Letharia* (Altermann et al. 2014), the *Parmotrema reticulatum* complex (Del-Prado et al. 2016), and *Pseudephebe* (Boluda et al. 2016). In some cases, a lack of correlation between genotypes and phenotypes has led to the recognition of cryptic species within morphologically indistinguishable or scarcely indistinguishable morphospecies (Molina et al. 2011a, b, Leavitt et al. 2012a, b, Singh et al. 2015, Boluda et al. 2016, Del-Prado et al. 2016), and so far, more than 80 cryptic lineages have been detected in *Parmeliaceae* (Crespo & Lumbsch 2010, Divakar et al. 2010). However, in other cases there is a mismatch between lineages revealed by standard DNA-barcoding markers and long-accepted morphospecies (Articus et al. 2002, Seymour et al. 2007, Velmala et al. 2014, Mark et al. 2016, Kirika et al. 2016a, b, McMullin et al. 2016).

In the morphologically similar ‘beard’ and ‘hair’ lichens of the *Alectoria sarmentosa*, *Bryoria* sect. *Implexae*, and *Usnea barbata* species complexes (Velmala et al. 2014, Mark et al. 2016, McMullin et al. 2016), DNA sequences from standard

¹ Departamento de Farmacología, Farmacognosia y Botánica (U.D. Botánica), Facultad de Farmacia, Universidad Complutense, Plaza de Ramón y Cajal s/n, Madrid 28040, Spain; corresponding author e-mail: Carlos G. Boluda, carlgala@ucm.es.

² Biodiversity and Conservation Biology, Swiss Federal Research Institute WSL, Zürcherstrasse 111, Birmensdorf 8903, Switzerland.

³ Botanical Museum, Finnish Museum of Natural History, P.O. Box 7, 00014 University of Helsinki, Finland.

⁴ Research and Collections, Canadian Museum of Nature, Ottawa, ON K1P 6P4, Canada.

⁵ Museum of Evolution, Uppsala University, Norbyvägen 16, 75236 Uppsala, Sweden.

⁶ Department of Life Sciences, The Natural History Museum, Cromwell Road, London SW7 5BD, UK; and Comparative Plant and Fungal Biology, Royal Botanic Gardens, Kew, Surrey TW9 3DS, United Kingdom.

Table 1 Specimen information and GenBank accession numbers of the *Bryoria* sect. *Implexae* samples used in this study. Newly obtained sequences are in **bold**.

Taxon	Locality	Source/Voucher	Lab. code	Fig. 2 and Appendix 4 code	Chemistry ¹	GenBank accession numbers					
						ITS	IGS	GAPDH	FRBi15	FRBi16	
<i>Bryoria capillaris</i>	Canary Islands, Tenerife	Veimala et al. (2014)	S192	87	Ale., Bar.	GQ996289	KJ396490	GQ996261	KY026810	KY002720	
	Canary Islands, Tenerife	MAF-Lich. 20683	L15.15	95	Ale., Bar.	KY026899	KY026945	KY026992	KY026807	KY002718	
	Finland, Etelä-Häme	Veimala et al. (2014)	L141	84	Ale., Bar.	FJ668493	FJ668455	FJ668399	KY026806	KY002697	
	Finland, Etelä-Savo	Veimala et al. (2014)	L211	85	Ale., Bar.	GQ996287	KJ396487	GQ996259	KY026809	KY002711	
	Finland, Uusimaa	Veimala et al. (2014)	S2	88	Ale., Bar.	KJ396433	KJ396489	KJ954306	KY026811	KY002729	
	Greece, Peloponnese	MAF-Lich. 19670	L06.10	91	Ale., Bar.	KY026894	KY026940	KY026987	KY026801	KY002715	
	Norway, Nord-Trøndelag	Veimala et al. (2014)	L270	86	Bar.	GQ996288	KJ396488	GQ996260	–	–	
	Spain, Lérida	MAF-Lich. 19672	L07.15	90	Ale., Bar.	KY026895	KY026941	KY026988	KY026802	KY002716	
	Spain, Madrid	MAF-Lich. 19664	L01.17	89	Ale., Bar.	KY026893	KY026939	KY026986	KY026800	KY002694	
	Spain, Navarra	MAF-Lich. 19674	L08.12	92	Ale., Bar.	KY026896	KY026942	KY026989	KY026803	KY002695	
	Spain, Teruel	MAF-Lich. 20682	L14.02	94	Ale., Bar., Fum., Pso.	KY026898	KY026944	KY026991	KY026805	KY002717	
	Sweden, Västerbotten	MAF-Lich. 19685	L13.03	93	Ale., Bar.	KY026897	KY026943	KY026990	KY026804	KY002696	
	Switzerland, Bivio	MAF-Lich. 20687	L16.21	96	Ale., Bar., Nor., Pso.	KY026900	KY026946	KY026993	KY026808	KY002719	
	<i>B. friabilis</i>	Canada	Veimala et al. (2014)	L407	15	Gyr.	KJ396435	KJ396492	KJ954308	KY026812	KY002751
		Canada, British Columbia	Veimala et al. (2014)	KJ396434	14	Gyr.	KJ396434	KJ396491	KJ954307	–	–
	<i>B. furcellata</i>	Canada, British Columbia	MAF-Lich. 20602	fil_02	17	Gyr.	–	KY083555	–	–	–
		USA, Alaska	Veimala et al. (2014)	S395a	16	Gyr.	KJ576728	KJ396493	KJ599481	–	–
		Finland, Etelä-Savo	Veimala et al. (2014)	L147	–	Fum.	HQ402722	KJ396494	HQ402627	–	–
		Canada	Veimala et al. (2014)	S259	71	Fum.	KJ396441	KJ396506	KJ954313	–	–
Canada, Alberta		Veimala et al. (2014)	S256	70	Fum.	GQ996307	KJ396505	GQ996280	KY026825	KY002702	
Canada, Alberta		Veimala et al. (2014)	S260a	72	Fum.	KJ396442	KJ396507	KJ954314	–	–	
Canada, Alberta		Veimala et al. (2014)	S261	73	Fum.	KJ396443	KJ396509	KJ954315	–	–	
Canada, Alberta		Veimala et al. (2014)	S267	74	Fum.	KJ576716	KJ396510	KJ599469	–	–	
Canada, Alberta		Veimala et al. (2014)	S272	75	Fum.	KJ576717	KJ396511	KJ599470	–	–	
Canada, Alberta		Veimala et al. (2014)	S369	77	Fum.	KJ396444	KJ396514	KJ954316	–	–	
<i>B. fuscescens</i>	Canada, Alberta	Veimala et al. (2014)	S379	78	Fum.	KJ396445	KJ396515	KJ954317	–	–	
	Canada, Alberta	Veimala et al. (2014)	S380	79	Fum.	KJ396446	KJ396516	KJ954318	–	–	
	Canada, Alberta	Veimala et al. (2014)	S274	76	Abs.	GQ996303	KJ396512	GQ996276	–	–	
	Canada, Alberta	MAF-Lich. 20684	L15.21	83	Fum.	KY026901	KY026949	KY026996	KY026817	KY002698	
	Canada, Alberta	Veimala et al. (2014)	L149	61	Fum.	GQ996290	KJ396496	GQ996262	KY026816	–	
	Canada, Alberta	Veimala et al. (2014)	L139	60	Fum.	KJ396436	KJ396495	KJ954309	KY026815	–	
	Canada, Alberta	Veimala et al. (2014)	S24	69	Fum.	KJ576715	KJ396501	KJ599468	KY026824	–	
	Canada, Alberta	Veimala et al. (2014)	S56	80	Fum.	GQ996291	KJ396502	GQ996263	–	KY002732	
	Canada, Alberta	Veimala et al. (2014)	L189	63	Fum.	GQ996305	KJ396498	GQ996278	KY026819	KY002699	
	Canada, Alberta	Veimala et al. (2014)	S109	67	Fum.	KJ396440	KJ396503	KJ954312	KY026822	KY002701	
	Greenland	Veimala et al. (2014)	L232	65	Abs.	GQ996304	KJ396500	GQ996277	–	KY002700	
	Norway, Sogn og Fjordane	Veimala et al. (2014)	L224	64	Fum.	KJ396437	KJ396499	KJ954310	KY026820	KY002731	
	Norway, Telemark	Veimala et al. (2014)	L305	66	Fum.	KJ396438	–	–	KY026821	–	
	Norway, Troms	MAF-Lich. 19681	L12.03	81	Fum.	KY026902	KY026947	KY026994	KY026813	–	
	Norway, Troms	MAF-Lich. 19682	L12.05	82	Fum.	KY026903	KY026948	KY026995	KY026814	KY002730	
	Russia, Perm Territory	Veimala et al. (2014)	S157	68	Fum.	GQ996306	KJ396504	GQ996279	KY026823	KY002742	
	Sweden, Södermanland	Veimala et al. (2014)	L160	62	Fum.	GQ996300	KJ396497	GQ996272	KY026818	–	
	<i>B. glabra</i>	Chile, IX Region	MAF-Lich. 20595	Bg1	5	Fum.	KY026904	KY026950	KY026997	–	–
		Chile, IX Region	MAF-Lich. 20596	Bg2	6	Fum.	KY026905	KY026951	KY026998	–	KY002693
Chile, IX Region		MAF-Lich. 20597	Bg3	7	Fum.	KY026906	KY026952	KY026999	–	KY002691	
Chile, IX Region		MAF-Lich. 20598	Bg4	8	Fum.	KY026907	KY026953	KY027000	–	–	
Chile, IX Region		MAF-Lich. 20599	Bg5	9	Fum.	KY026908	KY026954	KY027001	–	KY002690	
Finland, Koillismaa		Veimala et al. (2014)	L186	1	Abs.	FJ668494	FJ668456	FJ668400	–	KY002688	
USA, Alaska (epitype)		<i>Dillman 11May11:1</i> (UBC)	L406	2	Abs.	KY026909	KY083556	KY026955	–	KY002692	

Table 1 (cont.)

Taxon	Locality	Source/Voucher	Lab. code	Fig. 2 and Appendix 4 code	Chemistry ¹	GenBank accession numbers					
						ITS	IGS	GAPDH	FRB15	FRB16	
<i>B. glabra</i> (cont.)	USA, Alaska	<i>Dillman 26/July11:4</i> (UBC)	L414	3	Abs.	KY026910	KY083557	KY026956	—	—	
	USA, Washington	<i>Björk 1546</i> (UBC)	S388	4	Fum.	KY026911	—	—	—	KY002689	
<i>B. implexa</i>	Cyprus, Troodos	MAF-Lich. 19683	L11.15	105	Pso.	KY026915	KY026960	KY027005	KY026829	KY002704	
	Finland, Koillismaa	Veimala et al. (2014)	S22	98	Pso.	GO996294	KJ396517	GO996266	GO996266	KY026832	
	Finland, Koillismaa	Veimala et al. (2014)	S36	99	Pso.	KJ576719	KJ396518	KJ599472	KJ599472	KY026833	
	Finland, Koillismaa	Veimala et al. (2014)	S39	100	Pso.	GO996293	KJ396519	GO996265	GO996265	KY026834	
	Finland, Koillismaa	Veimala et al. (2014)	S67	101	Pso.	KJ396447	KJ396520	KJ954319	KJ954319	KY026835	
	Greece, Peloponnese	MAF-Lich. 19669	L06.05	103	Fum., Pso.	KY026913	KY026958	KY027003	KY026827	—	
	Morocco, Rif	MAF-Lich. 19679	L10.03	104	Pso.	KY026914	KY026959	KY027004	KY026828	KY002721	
	Russia, Murmansk	Veimala et al. (2014)	S168	97	Pso.	KJ396448	KJ396521	KJ954320	KY026831	KY002705	
	Spain, Madrid	MAF-Lich. 19663	L01.01	102	Pso.	KY026912	KY026957	KY027002	KY026826	KY002703	
	Switzerland, Bivio	MAF-Lich. 20685	L16.15	106	Pso.	KY026916	KY026961	KY027006	KY026830	—	
	<i>B. inactiva</i>	Canada, British Columbia	Veimala et al. (2014)	L206	18	Abs.	GO996283	KJ396522	GO996255	—	KY002760
		Canada, British Columbia	Veimala et al. (2014)	L323b	19	Abs.	KJ396449	KJ396523	KJ954321	KY026836	—
		Canada, British Columbia	Veimala et al. (2014)	L358	21	Abs.	KJ396451	KJ396525	KJ954323	KY026838	—
		Canada, British Columbia	Veimala et al. (2014)	S239a	22	Abs.	GO996284	KJ396526	GO996256	KY026839	—
		Canada, British Columbia	Veimala et al. (2014)	S392a	24	Abs.	KJ396452	KJ396528	KJ954324	—	—
		Canada, British Columbia (holotype)	Veimala et al. (2014)	L347	20	Abs.	KJ396450	KJ396524	KJ954322	KY026837	KY002761
USA, Alaska		Veimala et al. (2014)	S384	23	Abs.	KJ576724	KJ396527	KJ599479	—	—	
USA, Alaska (holotype)		Veimala et al. (2014)	L394	10	Pso.	KJ396453	KJ396529	KJ954325	KY026840	KY002764	
USA, Alaska		Veimala et al. (2014)	L396	11	Pso.	KJ396454	KJ396530	KJ954326	KY026841	KY002765	
<i>B. kuummerleana</i>		Iran, East Azarbaijan	Veimala et al. (2014)	L244a	107	Nor.	GO996295	KJ396531	GO996267	KY026846	—
	Morocco, Middle Atlas	MAF-Lich. 19677	L09.04	113	Nor.	KY026918	KY026963	KY027008	KY026843	KY002743	
	Morocco, Middle Atlas	MAF-Lich. 19678	L09.07	114	Nor.	KY026919	KY026964	KY027009	KY026844	KY002744	
	Norway, Nord-Trøndelag	Veimala et al. (2014)	L274	108	Nor.	GO996296	KJ396532	GO996268	KY026847	—	
	Norway, Nord-Trøndelag	Veimala et al. (2014)	L275	109	Nor.	KJ396455	KJ396533	KJ954327	—	—	
	Russia, Perm Territory	Veimala et al. (2014)	S160	111	Nor.	KJ396456	KJ396535	KJ954328	KY026849	—	
	Spain, Zamora	MAF-Lich. 19667	L04.03	112	Nor.	KY026917	KY026962	KY027007	KY026842	KY002706	
	Sweden, Härjedalen	Veimala et al. (2014)	S128	110	Nor.	KJ576720	KJ396534	KJ599473	KY026848	—	
	Switzerland, Bivio	MAF-Lich. 20686	L16.17	115	Nor., Pso.	KY026920	—	KY027010	KY026845	—	
	<i>B. pikeyi</i>	Canada, Alberta	Veimala et al. (2014)	S382	34	Ale., Bar.	KJ396466	KJ396547	KJ954338	KY026864	KY002752
		Canada, Alberta	Veimala et al. (2014)	S383a	35	Ale., Bar.	KJ396467	KJ396548	KJ954339	—	KY002759
		Canada, British Columbia	Veimala et al. (2014)	L197	25	Ale., Bar.	KJ396457	KJ396536	KJ954329	—	—
		Canada, British Columbia	Veimala et al. (2014)	L210	26	Ale., Bar.	KJ576714	KJ396539	KJ599467	—	KY002762
		Canada, British Columbia	Veimala et al. (2014)	L421	27	Ale.	KJ396462	KJ396543	KJ954334	KY026850	KY002753
		Canada, British Columbia	Veimala et al. (2014)	L374	28	Ale., Gyr.	KJ396459	KJ396540	KJ954331	KY026851	—
		Canada, British Columbia	Veimala et al. (2014)	L376	29	Ale., Gyr.	KJ396460	KJ396541	KJ954332	KY026852	KY002754
Canada, British Columbia		Veimala et al. (2014)	L377	30	Ale., Gyr.	KJ396461	KJ396542	KJ954333	KY026853	KY002755	
Canada, British Columbia		Veimala et al. (2014)	S221	31	Ale., Bar.	KJ396463	KJ396544	KJ954335	—	—	
Canada, British Columbia		Veimala et al. (2014)	S362	32	Ale., Bar.	KJ396464	KJ396545	KJ954336	—	—	
Canada, British Columbia		Veimala et al. (2014)	S368	33	Ale., Bar.	KJ396465	KJ396546	KJ954337	KY026863	KY002756	
Canada, British Columbia		MAF-Lich. 20601	plk_c	51	Ale.	—	—	—	—	—	
Canada, Nova Scotia		MAF-Lich. 20600	plk_a	49	Ale., Bar.	—	—	—	—	—	
Canada, Prince Edward Island		MAF-Lich. 20603	plk_02	38	Ale., Bar.	KY026925	KY026971	KY027014	KY026857	KY002749	
Canada, Prince Edward Island		MAF-Lich. 20606	plk_04	39	Ale., Bar.	KY026926	KY026972	KY027015	KY026858	KY002745	
Canada, Prince Edward Island		MAF-Lich. 20607	plk_05	40	Ale., Bar.	KY026927	KY026973	KY027016	KY026859	KY002727	
Canada, Prince Edward Island	MAF-Lich. 20609	plk_09	42	Ale., Bar.	—	—	—	—	KY002724		
Canada, Prince Edward Island	MAF-Lich. 20612	plk_10	43	Ale., Bar.	KY026921	KY026975	—	—	—		

Table 1 (cont.)

Taxon	Locality	Source/Voucher	Lab. code	Fig. 2 and Appendix 4 code		Chemistry ¹	GenBank accession numbers						
				ITS	IGS		GAPDH	FRB15	FRB16				
<i>B. pikei</i> (cont.)	Canada, Prince Edward Island	MAF-Lich. 20610	plk_11	44		Ale., Bar.	KY026922	KY026966	KY027011	KY026854	FRB16	KY002750	
	Canada, Prince Edward Island	MAF-Lich. 20622	plk_12	45		Ale., Bar.	–	KY026967	–	–	–	–	
	Canada, Prince Edward Island	MAF-Lich. 20611	plk_13	46		Ale., Bar.	KY026923	KY026968	KY027012	KY026855	–	KY002726	
	Canada, Prince Edward Island	MAF-Lich. 20613	plk_14	47		Ale., Bar.	KY026924	KY026969	KY027013	KY026856	–	KY002728	
	Canada, Prince Edward Island	MAF-Lich. 20614	plk_d	52		Ale., Bar.	–	–	–	–	–	KY002725	
	Canada, Quebec	MAF-Lich. 20608	plk_07	41		Ale., Bar.	–	KY026974	KY027017	KY026860	–	KY002723	
	Canada, Quebec	MAF-Lich. 20605	plk_15	48		Ale., Bar.	–	KY026970	–	–	–	KY002741	
	Canada, Quebec	MAF-Lich. 20604	plk_b	50		Ale., Bar.	KY026928	–	KY027018	KY026862	–	KY002748	
	USA, Alaska	Veimala et al. (2014)	S390	36		Ale., Bar.	KJ396468	KJ396549	KJ954340	–	–	–	
	USA, Oregon	Veimala et al. (2014)	S394	37		Ale., Bar.	KJ576727	KJ396550	KJ599480	–	–	–	
	<i>B. pseudofuscescens</i>	Canada, British Columbia (epitype)	Veimala et al. (2014)	S222	53		Nor.	KJ396469	KJ396551	KJ954341	KY026865	–	KY002757
		Canada, British Columbia	Veimala et al. (2014)	S232	54		Nor.	KJ396470	KJ396552	KJ954342	KY026866	–	–
		Canada, British Columbia	Veimala et al. (2014)	S370	55		Nor.	KJ396471	KJ396553	KJ954343	–	–	
Canada, British Columbia		Veimala et al. (2014)	S371	56		Nor.	KJ396472	KJ396554	KJ954344	–	–		
USA, Alaska		Veimala et al. (2014)	S377	57		Nor.	KJ396473	KJ396555	KJ954345	–	–		
USA, Alaska		Veimala et al. (2014)	S386	58		Nor.	KJ576725	KJ396556	KJ599478	–	–	KY002707	
USA, Alaska		Veimala et al. (2014)	S387	59		Nor.	KJ576726	KJ396557	KJ599477	KY026867	–	KY002758	
<i>B. sp.</i>		USA, Alaska	Veimala et al. (2014)	L395	12		Abs.	KJ396486	KJ396581	KJ954358	KY026869	–	KY002766
		USA, Alaska	Veimala et al. (2014)	L392	13		Abs.	KJ396485	KJ396580	KJ954357	KY026868	–	KY002763
<i>B. vrangiana</i>		Canada, Alberta	Veimala et al. (2014)	S385	124		Fum.	KJ396484	KJ396578	KJ954356	KY026886	–	KY002739
	Finland, Kainuu	Veimala et al. (2014)	S341b	123		Abs.	KJ396483	KJ396577	KJ954355	KY026885	–	–	
	Finland, Kainuu	Veimala et al. (2014)	S72	131		Abs.	KJ396481	KJ396573	KJ954353	KY026892	–	KY002740	
	Finland, Kollismaa	Veimala et al. (2014)	S10	119		Gyr.	GQ996297	KJ396564	GQ996269	KY026882	–	–	
	Finland, Kollismaa	Veimala et al. (2014)	S42	125		Gyr.	KJ396478	KJ396566	KJ954350	KY026887	–	KY002710	
	Finland, Kollismaa	Veimala et al. (2014)	S45	126		Abs.	GQ996302	KJ396568	GQ996275	KY026888	–	–	
	Finland, Kollismaa	Veimala et al. (2014)	S57	127		Fum.	KJ576722	KJ396570	KJ599475	–	–	–	
	Finland, Kollismaa	Veimala et al. (2014)	S59	128		Fum.	KJ396480	KJ396571	KJ954352	KY026889	–	–	
	Finland, Oulun Pohjanmaa	Veimala et al. (2014)	S196a	122		Abs.	KJ396482	KJ396576	KJ954354	KY026884	–	–	
	Finland, Uusimaa	Veimala et al. (2014)	S6	130		Fum.	KJ396477	KJ396563	KJ954349	KY026890	–	–	
	Finland, Varsinais-Suomi	Veimala et al. (2014)	S62	129		Gyr.	KJ576721	KJ396572	KJ599474	KY026891	–	–	
	Italy, Sicily	MAF-Lich. 19668	L05.17	135		Fum.	KY026931	KY026978	KY027021	KY026872	–	KY002709	
	Morocco, Rif	MAF-Lich. 19680	L10.13	140		Abs.	KY026936	KY026983	KY027026	KY026877	–	KY002722	
	Norway, Nord-Trøndelag	Veimala et al. (2014)	L272	116		Gyr.	GQ996299	KJ396558	GQ996271	KY026870	–	KY002727	
	Norway, Nord-Trøndelag	Veimala et al. (2014)	L273	117		Abs.	KJ396474	KJ396559	KJ954346	KY026880	–	KY002747	
	Norway, Nord-Trøndelag	Veimala et al. (2014)	L300	118		Abs.	GQ996301	KJ396562	GQ996274	–	–	–	
	Norway, Oppland	Veimala et al. (2014)	L307	132		Gyr.	KJ396439	–	KJ954311	KY026881	–	KY002746	
	Norway, Troms	MAF-Lich. 19684	L12.11	141		Fum., Gyr.	KY026937	KY026984	KY027027	KY026878	–	KY002738	
Russia, Perm Territory	Veimala et al. (2014)	S164	120		Abs.	GQ996285	KJ396574	GQ996257	KY026883	–	KY002712		
Russia, Perm Territory	Veimala et al. (2014)	S166	121		Fum.	GQ996308	KJ396575	GQ996273	–	–	KY002713		
Spain, Asturias	MAF-Lich. 19666	L03.07	134		Fum.	KY026930	KY026977	KY027020	KY026871	–	KY002708		
Spain, Cáceres	MAF-Lich. 19665	L02.20	133		Fum.	KY026929	KY026976	KY027019	KY026870	–	KY002734		
Spain, Lérida	MAF-Lich. 19671	L07.03	136		Fum.	KY026932	KY026979	KY027022	KY026873	–	KY002735		
Spain, Lérida	MAF-Lich. 19673	L07.19	137		Abs.	KY026933	KY026980	KY027023	KY026874	–	KY002736		
Spain, Navarra	MAF-Lich. 19675	L08.19	138		Abs.	KY026934	KY026982	KY027024	KY026875	–	KY002737		
Sweden, Västerbotten	MAF-Lich. 19686	L13.12	142		Gyr.	KY026938	KY026985	KY027028	KY026876	–	KY002739		

¹ Abs. = No substances detected; Ale. = Aleoctic acid; Bar. = Barbatolic acid; Fum. = Fumarprotocetraric acid; Gyr. = Gyrophoric acid; Nor. = Norstictic acid; Pso. = Psoromic acid.

barcoding markers show that what were considered well delimited morphospecies are found admixed in a single lineage that may be interpreted as a single phylogenetic species. In such situations, many processes may be operative, including environmental plasticity (Boluda et al. 2016), hybridisation, ancestral polymorphisms, incomplete lineage sorting (Joly et al. 2009), limited value of neutral markers (Bekessy et al. 2003), or morphological variability mediated by low selective pressure, genetic drift, or huge population sizes (Hartl & Clark 2007). In these cases, the use of additional markers, especially highly variable ones (e.g., microsatellites), may contribute to an explanation of the underlying phenomena.

Chemical characters, mainly the production of polyketides, were accorded major importance in species delimitation in lichen-forming fungi in the 1960s and 1970s (Hawksworth 1976, Lumbsch 1988). These compounds are formed by the fungal partner, and that expression can differ according to the position in a thallus or in pure culture. For almost 50 years, chemical products, generally linked to minor morphological differences, have been used to circumscribe species in *Bryoria* (Hawksworth 1972, Brodo & Hawksworth 1977, Myllys et al. 2011, Velmala et al. 2014). The advent of molecular phylogenetics has enabled such species concepts to be tested, and they have proved particularly wanting in one group of species, those placed in *Bryoria* sect. *Implexae* (Myllys et al. 2011, Velmala et al. 2014, Boluda et al. 2015). Velmala et al. (2014) provided DNA sequence data for 11 species in the section, and with the exception of *B. glabra*, all the other species were intermixed in clades with diverse, and not concordant, chemical and morphological features. Genetically indistinguishable taxa (with the markers used), maintain distinctive phenotypes even when growing in physical contact with one another (Velmala et al. 2014, Boluda et al. 2015), so the variation cannot be attributed solely to ecological factors.

A study on the morphospecies *B. fuscescens* in central Spain (Boluda et al. 2015) revealed specimens with the same nuclear internal transcribed spacer sequence (nuITS) but different exrolites (compounds formed on the surface of or excreted from hyphae). Subsequent fieldwork across Europe has revealed further combinations of exrolites, and also specimens sharing characters of additional morphospecies. In order to understand the evolutionary processes involved in *B. fuscescens* and related species we have adopted an integrative approach including morphological, distributional, and chemical data together with DNA sequences from three standard loci (Schoch et al. 2012), two newly tested loci, and eighteen microsatellite (SSRs) markers (Nadyeina et al. 2014). We then analysed these datasets in a rigorous statistical framework to effectively integrate an evolutionary perspective into a revised and defensible taxonomic treatment. These studies are reported here, and we anticipate that the experience gained in this group of lichens will inform how other species complexes with similarly discordant datasets can be addressed.

MATERIALS AND METHODS

Sampling

We examined 142 specimens from 14 countries in Europe, the Mediterranean Basin, and North and South America, representing 11 named morphospecies in *Bryoria* sect. *Implexae* (Table 1). Our dataset included 91 of the 97 specimens used by Velmala et al. (2014) in their revision of *B. sect. Implexae*. Newly obtained sequences are shown in **bold** in Table 1. *Bryoria furcellata* was used as outgroup to root the tree (Velmala et al. 2014). Names used in the analyses follow the species concepts adopted in Velmala et al. (2014).

Morphology and chemistry

The newly studied specimens (Table 1) were examined morphologically under a Nikon SMZ-1000 dissecting microscope, and hand-cut sections studied with a Nikon Eclipse-80i compound microscope equipped with bright field and differential interference contrast (DIC). Habit photographs were taken with a Nikon 105 mm f/2.8D AF Micro-Nikkor Lens coupled to a Nikon D90 camera with daylight. Spot tests (K, C, and PD) and TLC were carried out following Orange et al. (2010). Solvent system C (200 ml toluene / 30 mL acetic acid) was used for TLC, with concentrated acetone extracts at 50 °C spotted onto silica gel 60 F254 aluminium sheets (Merck, Darmstadt, Germany). Spotted sheets were dried for 10 min in an acetic acid atmosphere to maximize resolution. Segments from the same lichen branch were used for both TLC and DNA extraction to avoid the possible risk of taking samples from mixed collections. Morphological and thin layer chromatographic (TLC) analyses of the samples used in Velmala et al. (2014; Table 1) were taken from that study.

DNA dataset

The molecular dataset comprised DNA sequences and SSRs frequencies. DNA extraction was performed with the DNeasy Plant Mini Kit (Qiagen, Barcelona, Spain), following the manufacturer's instructions.

Eighteen fungal-specific microsatellites markers (Bi01, Bi02, Bi03, Bi04, Bi05, Bi06, Bi07, Bi08, Bi09, Bi10, Bi11, Bi12, Bi13, Bi14, Bi15, Bi16, Bi18 and Bi19) were amplified following Nadyeina et al. (2014) using fluorescently labelled primers. Fragment lengths were determined on an ABI PRISM® 3130 Genetic Analyser (Life Technologies, Carlsbad, CA, USA). Genotyping was performed using GeneScan-500 LIZ as the internal size standard and GeneMapper v. 3.7 (Applied Biosystems, Foster City, CA, USA).

For DNA sequencing, five loci were selected (Table 2), three commonly used as standard markers in fungi (ITS, IGS, and *GAPDH*), which were also used in Velmala et al. (2014), and two microsatellite flanking regions tested here for the first time

Table 2 Primer information used in *Bryoria* sect. *Implexae*.

Marker	Description	Primer forward (5'–3')	Source	Primer reverse (5'–3')	Source
ITS	Internal transcribed spacers of the nuclear rDNA including the 5.8S region	ITS1-F: CTTGGTCATTAGAGGAAGTAA	Gardes & Bruns (1993)	ITS4: TCCTCCGCTTATTGATATGC	White et al. (1990)
IGS	Intergenic spacer of the nuclear rDNA	IGS12b: AGTCTGTGGATTAGTGCCCG	Printzen & Ekman (2002)	SSU72R: TTGCTTAAACTTAGACATG	Gargas & Taylor (1992)
<i>GAPDH</i>	Glyceraldehyde 3-phosphate dehydrogenase gene partial sequence	Gpd1-LM: ATTGGCCGCATCGTCTCCGCAA	Myllys et al. (2002)	Gpd2-LM: CCACTCGTTGTCGTACCA	Myllys et al. (2002)
FRBi15	Flanking region of <i>Bryoria</i> sect. <i>Implexae</i> microsatellite marker 15	FRBi15f: GTCATAAGGGTATCAATCC	This paper	FRBi15r: TGAAAAGGTTTGGTGACTC	This paper
FRBi16	Flanking region of <i>Bryoria</i> sect. <i>Implexae</i> microsatellite marker 16	FRBi16f: CGAGGTTTCAGGAAAGGAA	This paper	FRBi16r: AGGAAGTGATGTCGAGGT	This paper

(FRBi15 and FRBi16). Microsatellite flanking regions are variable non-coding DNA fragments that can contain phylogenetic signal through a neutral molecular evolution (Zardoya et al. 1996, Chatrou et al. 2009). To explore this possibility, the flanking regions of the 18 microsatellite markers were checked upstream and downstream in the 454 pyrosequencing contigs used for microsatellite searching in Nadyeina et al. (2014). The variability of each region was assessed with the number of variable sites in contigs supported by 2–16 copies. From the 36 regions (two for each of the 18 microsatellites), the most variable flanking regions were in Bi15 and Bi16, and specific primers were designed for those loci (Table 2).

New DNA sequences (Table 1) were obtained using polymerase chain reactions (PCRs) as follows: a reaction mixture of 25 μ L, containing 12 μ L sterile water, 9 μ L JumpStart™ REDTaq ReadyMix PCR Reaction Mix (Sigma-Aldrich, St Louis, MI, USA), 1.25 μ L of each primer (forward and reverse) at 10 μ M, and a 1.5 μ L DNA template. Cycling conditions for ITS, *GAPDH*, FRBi15, and FRBi16 were 2 min at 94 °C; 35 cycles of 30 s at 94 °C; 30 s at 56 °C; 2 min at 72 °C; and a final extension of 5 min at 72 °C. For IGS, the cycling process was: 2 min at 94 °C; 15 cycles of 30 s at 94 °C, 30 s at 55 °C (decreasing 1 °C each cycle down to 40 °C), 2 min at 72 °C, then 35 cycles of 30 s at 94 °C, 30 s at 55 °C; 90 s at 72 °C, and a final extension of 5 min at 72 °C. PCR products were checked and quantified on 1 % agarose gel stained with ethidium bromide and cleaned using Exonuclease I and FastAP Thermosensitive Alkaline Phosphatase (Thermo Fisher Scientific, Waltham, MA, USA) according to the manufacturer's instructions. Sequencing was performed with labelling using BigDye Terminator v. 3.1 Kit (Applied Biosystems) as follows: 25 cycles of 20 s at 96 °C, 5 s at 50 °C, and 2 min at 60 °C. PCR products were cleaned-up with the BigDye XTerminator Purification Kit (Applied Biosystems) according to the manufacturer's instructions. Sequences were obtained in an ABI PRISM 3130 Genetic Analyser (Life Technologies) and manually adjusted using DNA Workbench v. 6 (CLC bio, Aarhus, Denmark) and MEGA5 (Tamura et al. 2011). Newly generated sequences were deposited in GenBank (Table 1 in **bold**).

Clustering methodologies

Phenetic analyses

Two presence/absence (1/0) matrices were constructed, one for the extrolites detected by TLC, and another with morphology and geography data (Appendix 1). Morphological characters scored comprised those traditionally used to separate morphospecies in the group:

1. pale/dark thallus colour;
2. branching angles (acute/obtuse/mixed);
3. soralia (absent/fissural/tuberculate/both); and
4. pseudocyphellae (conspicuous/inconspicuous).

For distributions, Old World vs New World was used. The R package cluster (Maechler et al. 2013) was used to obtain the dissimilarity matrix, and then the pvclust package (Suzuki & Shimodaira 2006) was run to obtain a phenogram (Zamora et al. 2013). Multiscale bootstrap resampling with 10 000 bootstrap (bp) replicates was used to obtain approximately unbiased (au) p-values for branch supports. Groups were considered as supported when bp values exceeded 70 or au values exceeded 95.

Phylogenetic tree

Alignments for each locus were performed using MAFFT v. 7 (<http://mafft.cbrc.jp/alignment/server/>; Katoh & Standley 2013) with the G-INS-i alignment algorithm, a '1PAM/K = 2' scoring matrix, with an offset value of 0.1, and the remaining parameters set as default. Alignments were deposited in TreeBASE

under accession nos TB2:S20007 (ITS, IGS, and *GAPDH*), TB2:S20005 (FRBi15), and TB2:S20004 (FRBi16). RDP v. 4 (Martin et al. 2010) was used to detect potential recombination events, through the methods RDP (Martin & Rybicki 2000), GENECONV (Padidam et al. 1999), Chimaera (Posada & Crandall 2001), Maxchi (Maynard-Smith 1992), Bootscan (Gibbs et al. 2000, Martin et al. 2005), SiScan (Weiller 1998, Gibbs et al. 2000), PhyPro (Weiller 1998), and 3Seq (Boni et al. 2007). Partitionfinder (Lanfear et al. 2012) was used to detect possible intra-locus substitution model variability, resulting in the splitting of the ITS region into ITS1, 5.8S, and ITS2, and coding each codon position separately in *GAPDH*. Models of DNA sequence evolution for each locus partition were selected with jModeltest v. 2.0 (Darriba et al. 2012), using the Akaike information criterion (AIC, Akaike 1974). The best-fit model of evolution obtained was: ITS1 = TIM2, 5.8S = K80, ITS2 = TIM2ef + G, IGS = TrN + I, *GAPDH* 1st position = TrN + I, *GAPDH* 2nd position = F81 + I, *GAPDH* 3th position = TPM3uf, FRBi15 = TPM3uf + I, FRBi16 = TPM3uf + G. To detect possible topological conflicts among loci, the CADM test (Legendre & Lapointe 2004, Campbell et al. 2011) was performed using the function 'CADM.global' implemented in the library 'ape' of R (Paradis et al. 2004). As loci FRBi15 and FRBi16 were not congruent among them and neither with the remaining loci, three alignments were used, resulting in three trees, one for each FRBi region and another for the concatenated dataset including loci ITS, IGS and *GAPDH*. For the concatenated matrix, specimens with more than one missing locus were excluded. Datasets were analysed using maximum likelihood (ML) and Bayesian (B/MCMCMC) approaches with gaps treated as missing data.

For ML tree reconstruction, we used RAXML v. 8.2.10 (Stamatakis 2006) implemented in CIPRES Science Gateway (<https://www.phylo.org/>; Miller et al. 2010) with the GTRGAMMA model (Stamatakis 2006, 2014, Stamatakis et al. 2008). Support values were assessed using the 'rapid bootstrapping' option with 1000 replicates. For the Bayesian reconstruction, MrBayes v. 3.2.1 (Ronquist & Huelsenbeck 2003) was used. Two simultaneous runs with 10 M generations each, starting with a random tree and employing 12 simultaneous chains, were executed. Every 500th tree was saved to a file. Preliminary analysis resulted in an overestimation of branch lengths and to correct this we used the uniform compound Dirichlet prior brlenspr = unconstrained : gammadir (1, 1, 1, 1; Zamora et al. 2015). We plotted the log-likelihood scores of sample points against generations using Tracer v. 1.5 (Rambaut et al. 2014) and determined that stationarity had been achieved when the log-likelihood values of the sample points reached an equilibrium and ESS values exceeded 200 (Huelsenbeck & Ronquist 2001). Posterior probabilities (PPs) were obtained from the 50 % majority rule consensus of sampled trees after excluding the initial 25 % as burn-in. The phylogenetic tree was drawn with FigTree v. 1.4 (Rambaut 2009).

STRUCTURE

STRUCTURE v. 2.3.4 (Pritchard et al. 2000, Falush et al. 2003) was run with the SSRs data matrix. Analysis was computed with 100 000 burn-in generations and 100 000 iterations using a K value from 1 to 12 (i.e., the putative number of species we may have) and 20 replicates for each K. To combine the 20 runs of each K in a single result, CLUMMP v. 1.1.2 (Jakobsson & Rosenberg 2007) was used and visualised replacing the CLUMMP output values in a STRUCTURE output of the same K, and then plotted using the STRUCTURE software. To show the probability of each K value, STRUCTURE HARVESTER (Earl & Von Holdt 2012), with the ΔK method (Evanno et al. 2005) was used, considering the most probable K the first one that appears close to 0 in the output graphic.

Principal coordinate analysis

Principal coordinate analysis (PCoA) was carried out with the SSRs length data in GenAlEx 6.5. The results of the three first axes were plotted in a three-axis graph using The Excel 3D Scatter Plot v. 2.1, in which the graphic can be moved in 3D to obtain a better understanding of how the plots are distributed in the space. Since the projection of this 3D graph on a paper is necessarily confusing, PCoA results were plotted on two different 2D graphs showing axes 1 and 2, and 1 and 3, respectively.

Haplotype network

Haplotype network reconstruction was performed using TCS v. 1.2.1 (Clement et al. 2000) with the concatenated sequences matrix, excluding the outgroup, using gaps as missing data, and a 95 % connection limit. Specimens differing only by missing or ambiguous characters were not counted as haplotypes.

Species delimitation analyses

In order to examine species delimitation, four computational approaches not requiring prior hypothesis of a putative number of species were used:

1. Automatic Barcode Gap Discovery ABGD (Puillandre et al. 2011) based on barcode gaps using genetic distances;
2. Poisson Tree Processes PTP (Zhang et al. 2013), based on gene trees;
3. The Generalized Mixed Yule coalescent approach GMYC, which combines a coalescent model of intraspecific branching with a Yule model for interspecific branching (Pons et al. 2006, Monaghan et al. 2009); and
4. DISSECT (Jones et al. 2014) based on the multispecies coalescent model for species delimitation.

ABGD and PTP were carried out using the online servers <http://www.wabi.snv.jussieu.fr/public/abgd/> and <http://species.h-its.org>, respectively. GMYC was analysed with the `gmyc` function in the SPLITS package in R (v. 2.10, www.cran.r-project.org), employing the single (GMYCs) and multiple (GMYCm) threshold methods. Because GMYC needs a strictly ultrametric and bifurcating tree with no zero branch lengths, identical sequences were deleted and an ultrametric tree was generated using BEAST v. 1.8.2 software (Drumond et al. 2012), with the evolutionary models explained in the Bayesian phylogenetic reconstruction. A run of 100 M iterations logging every 1 000th iteration was conducted. Consensus tree was generated with TreeAnnotator v. 1.8.2 after discarding the initial 10 % trees as burn-in. ESS values above 200 were ensured using Tracer v. 1.6 (Rambaut et al. 2014).

DISSECT analysis was implemented in STARBEAST (*BEAST, Drumond et al. 2012) using the concatenated DNA matrix after removing identical sequences and following the instructions of Jones et al. (2014). First, we used BEAUti (Drumond et al. 2012) to produce the xml file, with every individual encoded as if it was a separate species. Sites, clocks and trees were released as unlinked. Nucleotide substitution models and other parameters (as in the Bayesian analysis, see above), were encoded using BEAUti if possible, or manually entered. For the ITS locus, a substitution rate of 0.0033 substitutions per site per million years was introduced (Leavitt et al. 2012a, b), setting other loci as estimated with a lognormal relaxed clock. A birth-death-collapse prior that controlled the minimal split heights for the putative resulting species was manually added to the xml file. This prior contained the parameters CollapseHeight (ϵ) with a value of 0.0001 and CollapseWeight (ω), set as estimated using a Beta distribution with values 10 and 1.5. Selected parameters provide a highest probability density around 4–5 clusters, the most probable number of taxa meriting separation according to other analyses performed for this paper. However, this prior is diffuse and allows to obtain a different number of putative taxa if they

adjust better to the data. The xml file was executed in BEAST with 250 M MCMC iterations, sampling every 10 000th iteration. Tracer v. 1.6 (Rambaut et al. 2014) was used to assess ESS values above 140. The resulting *BEAST species tree output was then treated with SpeciesDelimitationAnalyzer (Jones et al. 2014), with a burn-in of 5 000 trees (20 % of the total generated), a collapse height of 0.001 (one fraction lower than in the *BEAST analysis) and a simcutoff value of 1 to ignore this parameter, as according to sequence variability, we expected very similar putative species to emerge. The resulting similarity matrix was plotted with R v. 2.15.1 (R Core Team 2014) following the method of Jones et al. (2014).

Divergence time estimation

Two divergence time estimations were performed, one only with the ITS region and a defined substitution rate, and the other with the concatenated data matrix of ITS, IGS, and *GAPDH* loci. A rate of 3.30×10^{-9} s-s⁻¹-yr⁻¹ for the ITS region as a whole was used, with a GTR + G + I substitution model (Leavitt et al. 2012a, b). In the concatenated matrix analysis, as no previous literature on substitution rates for IGS and *GAPDH* in lichen-forming fungi is available, these were set as estimated in the Bayesian phylogenetic analysis. A *BEAST analysis was executed, using a relaxed clock model (uncorrelated lognormal), a birth-death model prior for the node heights and unlinked substitution models, clocks and trees for each partition. Clades G, Ko, NA, and WD were selected as potential species, forcing them to remain monophyletic (Fig. 6). No calibration points could be used, as no fossils or previous dating of this species complex are available. To avoid stochastic events, two independent analyses were run, each with 200 million generations, sampling each 5 000 trees, and discarding the first 10 000 trees (25 %) as burn-in. Tracer v. 1.6 (Rambaut et al. 2014) was used to ensure ESS parameter values above 115 in the concatenated matrix, and 185 for the ITS analysis. Different priors were tested but no higher ESS values could be obtained, which we suspect was due to the very similar sequences, and the uncertain topology of the backbone connecting the groups Ko, NA, and WD. The two runs performed for each input were merged with logcombiner v. 1.8.2, and the resulting trees merged in a consensus tree using TreeAnnotator v. 1.8.2 (Drumond et al. 2012). FigTree v. 1.4 (Rambaut 2009) was used to display the ITS and the concatenated dated species trees.

Demography

Changes in population sizes through time were estimated using the Bayesian skyline analysis (Drumond et al. 2005) with BEAST. Only clades Ko, NA, and WD, isolated and merged, were studied, as they show a clock-like tree topology and adequate sampling sizes.

Following the methods used for divergence time estimation analysis, the demography analyses were run using the ITS region without partitioning, with the GTR + G + I model of nucleotide substitution and a substitution rate of 3.30×10^{-9} s-s⁻¹-yr⁻¹, and with a strict molecular clock model (Leavitt et al. 2012a, b). Additionally, the same analysis was repeated with the concatenated data matrix using the ITS substitution rate, estimating the other loci rates with a relaxed clock model and using the nucleotide substitution models for IGS and *GAPDH* explained in the Bayesian phylogenetic reconstruction. Four independent runs for each input were processed with 50 M MCMC generations, sampling parameter values every 5 000th generation, using the Bayesian Skyline tree prior model, six discreet changes in population size and the linear growth option. ESS values were checked with Tracer v. 1.5 (Rambaut et al. 2014), and the two best of the four runs were combined, obtaining values usually above 200, with some exceptions with a lower limit of 100. Skyline plots were drawn with Tracer v. 1.5.

To support the Bayesian skyline test, a neutrality test was performed to infer if populations are in mutation-drift equilibrium. Tajima's D (Tajima 1989) and Fu's Fs (Fu 1997) were calculated with DnaSP v. 5.10 (Librado & Rozas 2009). A significantly positive D is interpreted as a diversifying selection or a recent bottleneck, whereas a negative significant D shows purifying selection or a recent expansion. If D is not significantly different from 0, a mutation-drift equilibrium may be occurring. Fu's Fs can be interpreted in the same way.

RESULTS

Morphological and chemical clustering

The wide geographical range of collections revealed a combination of characters not previously reported in the *Bryoria fuscescens* complex, especially those from the previously less-studied Mediterranean Basin. Specimens with intermediate morphologies amongst traditionally accepted species were recognized, and the application of species names according to the current taxonomy was ambiguous. Individuals connecting the phenotypes and chemotypes of the taxa currently recognized as *Bryoria fuscescens*, *B. implexa*, *B. kuemmerleana*, and *B. vran-giana* were not rare in the Mediterranean Basin. For example, chemotypes thought to be diagnostic for a particular taxon were detected in specimens morphologically belonging to other

taxa, as well as specimens producing extrolites characteristic of different taxa in a single thallus. Thin-layer chromatography (TLC) revealed seven different extrolites: alectorialic, barbatolic, fumarprotocetraric, gyrophoric, norstictic, and psoromic acids, atranorin, and sometimes also related substances such as chloroatranorin, protocetraric, or connorstictic acids. Atranorin, a typical accessory substance in the genus *Bryoria*, was not used in the posterior analyses because it appears in trace amounts in many samples and is often difficult to unequivocally discern if it is present or absent by TLC alone.

The chemical presence/absence matrix resulted in the phenogram shown in Appendix 2a. The matrix included specimens with as many as four extrolites, something not previously reported in the complex. Chemical characters were separated into two main groups:

1. specimens that contain benzyldepsides (i.e., alectorialic and barbatolic acids), substances traditionally used to separate *B. capillaris* and *B. pikei* from other species in the complex; and
2. specimens without benzyldepsides.

The latter were clustered in two well-supported groups, one with fumarprotocetraric acid as the main substance, and the other without it (including specimens with no detectable substances). If the structural relationships of the compounds were encoded in the presence/absence matrix (benzyldepsides vs depsidones), the same clustering was obtained.

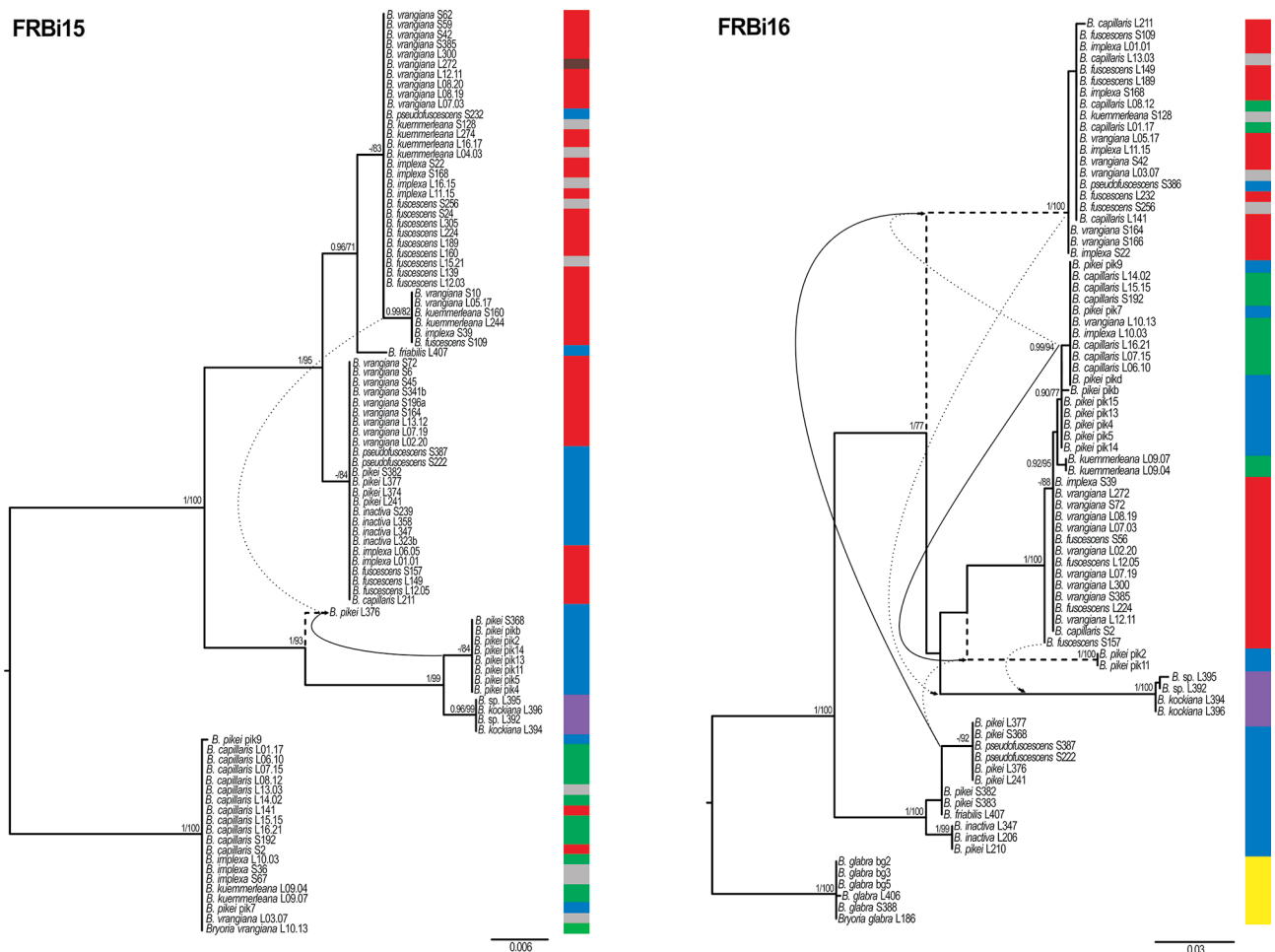


Fig. 1 Phylogenetic relationships in *Bryoria* sect. *Implexae* based on FRBi15 and FRBi16 loci. Tree topology depicts the result of the Bayesian Markov chain Monte Carlo (B/MCMC) analysis. Posterior probabilities and bootstrap analysis for the supported nodes (≥ 0.95 and $\geq 70\%$) are indicated at the main nodes. Lines connecting clades indicate putative recombination events, with main parents (continuous lines) and minor parents (discontinuous lines). Because the clade insertion in the trees is influenced by the recombination, clades with recombination are depicted with a discontinuous branch line. Note that clades with recombination appear as sister or close to the main parent but tending to be deviated towards the minor parent. — The coloured bar corresponds to the SSR genepool from Fig. 2, with specimens intermediate between two or more genepools in grey. The clades obtained, although well-supported, do not follow any evident geographic, morphologic, chemical, or microsatellite pattern.

The analysis of combined morphological, geographical, and chemical characters resulted in the phenogram in Appendix 2b. Only terminal branches were supported, including few monophyletic morphospecies, although not well isolated from others. Neither accepted morphospecies nor an unequivocal number of phenotypic groups could be recognized. This ambiguity was largely attributable to phenotypically intermediate specimens, mainly from the Mediterranean Basin, and also by the presence of some shared characters amongst the morphospecies, such as the presence/absence of soralia, pseudocyphellae, extrolite composition, and thallus colour.

Phylogenetic tree

Due to the topological conflict between loci, three DNA matrices were used to generate three phylogenetic trees:

1. a concatenated matrix including ITS, IGS, and *GAPDH* with 134 individuals consisting of 1774 unambiguously aligned nucleotide position characters, with 83 parsimony informative (Pi) sites;

2. FRBi15 with 93 individuals contained 569 unambiguously aligned nucleotide position characters, with 44 Pi sites; and
3. FRBi16 with 80 individuals had 632 unambiguously aligned nucleotide position characters, with 160 Pi sites.

No evidence of recombination events was detected in the concatenated matrix. The resulting tree (Fig. 6) had four well-supported main clades, G (Glabra, yellow), Ko (Kockiana, magenta), NA (North American, blue), and WD (Widely Distributed, red + green + brown). Clade G included only material of *B. glabra*, appearing as an isolated taxon sister to the other three clades, which showed an uncertain topology between them. Clade Ko included material named *B. kockiana* and two unidentified specimens, all collected in Alaska (USA). Clade NA comprised the previously recognized North American morphospecies group (the 'North American endemic species', Velmala et al. 2014) named as *B. friabilis*, *B. inactiva*, *B. pikei*, and *B. pseudofuscescens*. While these species were mixed in the tree, the group as a whole was resolved as monophyletic. The WD clade included specimens widely distributed but mainly from

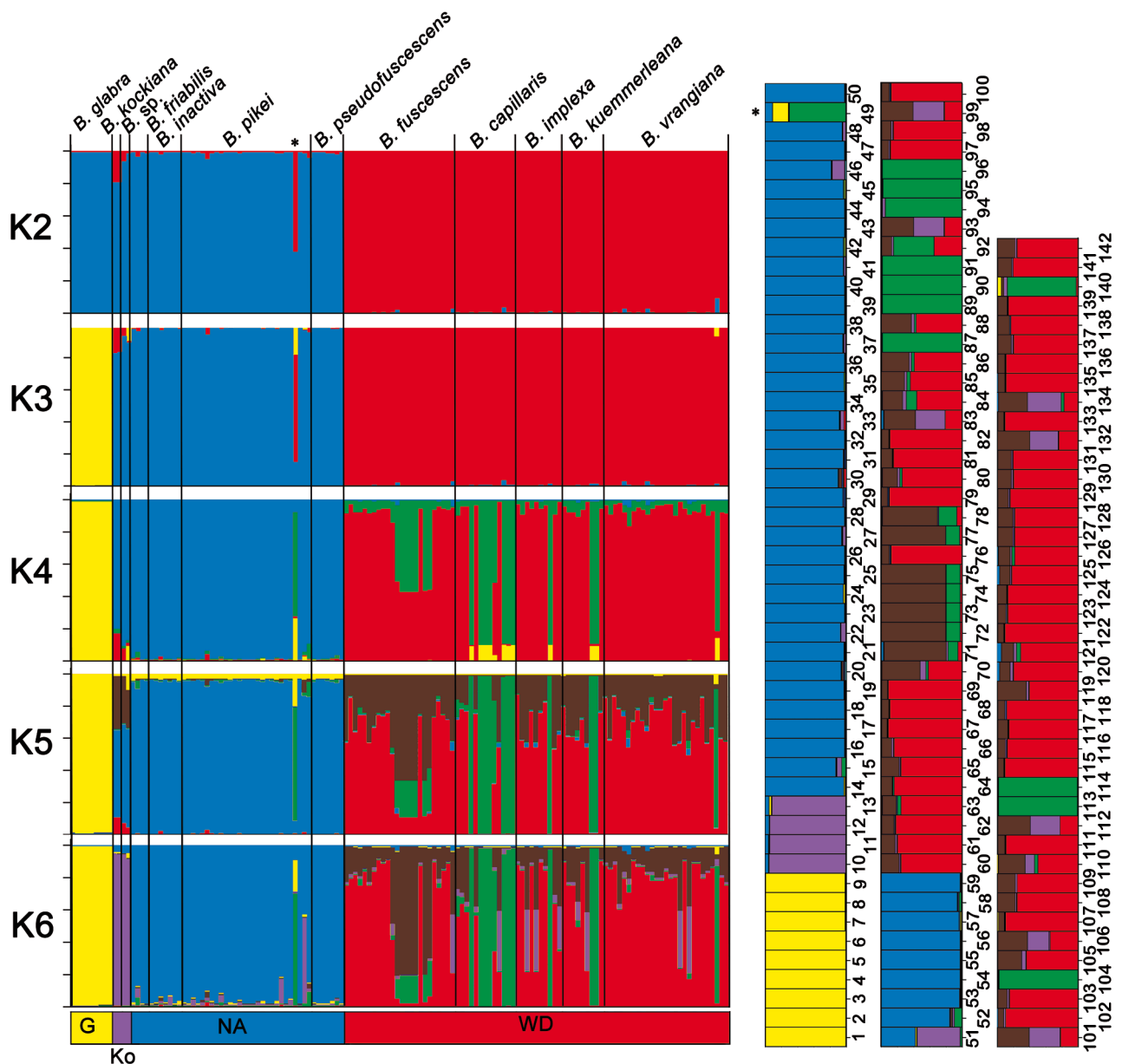


Fig. 2 Bayesian inference of population structuring using STRUCTURE v. 2.3.4 (Pritchard et al. 2000, Falush et al. 2003) and nine microsatellite loci in *Bryoria* sect. *Implexae*. – Left. Results from the hypothesis of 2–6 clusters. Vertical bars represent specimen assignment probability into a genetic cluster depicted by the colours. Morphospecies names given to the specimens appear at the top. – Right. Detailed columns of the K = 6 hypothesis, the numbers representing the specimens shown in Table 1 to provide a better understanding of the components of each individual. — G = Glabra clade; Ko = Kockiana clade; NA = North American clade; WD = Widely Distributed clade; * = *Bryoria pikei* specimen 49.

Europe (the ‘European and globally distributed species’ group, Velmala et al. 2014) under the names *B. capillaris*, *B. fuscescens* (syn. *B. chalybeiformis* and *B. lanestrus*), *B. implexa*, *B. kuemmerleana*, and *B. vrangiana*. None of these previously recognised species formed a monophyletic group.

The phylograms produced using the FRBi15 and FRBi16 markers had a different tree topology, not congruent among them or with that from the preceding concatenated dataset. In the FRBi15 reconstruction (Fig. 1), *B. glabra* was not represented due to the lack of primer annealing in the PCR process, and the tree could not be rooted. Several well-supported groups were produced, but did not follow any evident geographic, morphological, chemical, or SSR frequency pattern. *Bryoria pikei* L376 had a sequence with a putative recombination fragment with the *B. vrangiana* S10 clade in c. 50 % of the total length. This insertion placed the specimen out of the main parental group and it appears as its sister. Although marker FRBi16 (Fig. 1) also produced a well-resolved tree with supported nodes, the clades do not show any phenotypic and/or geographic structure. In this tree reconstruction, *B. glabra* was an isolated taxon and served to root the tree. In FRBi16 sequences, many putative recombination events were detected, suggesting a reticulate evolution. In both trees in Fig. 1, clade Ko (magenta) was recovered as monophyletic, but embedded between other named morphospecies.

STRUCTURE clustering

Of the 18 microsatellite markers, the nine that showed more than 95 % successful amplification across the samples were used (number of haplotypes shown in brackets, Appendix 3): Bi01 (17), Bi03 (6), Bi04 (8), Bi05 (5), Bi10 (8), Bi11 (9), Bi12 (12), Bi14 (6), and Bi19 (5). We allowed a maximum of three missing loci per specimen, a value reached only in seven samples. STRUCTURE was allowed to run to $K = 12$, but from $K = 6$ the clustering process started to be uninformative (Fig. 2). The likelihood results of the ΔK analysis (Evanno et al. 2005) indicated three as the most probable number of clusters (likelihood = -1232, $\Delta K = 2.2$), the clades G, NA, and WD (Fig. 2, $K = 3$). Clade Ko, which appeared isolated in the concatenated phylogenetic tree (Fig. 6), could not be accepted as distinct under a $K = 3$ hypothesis. However, *B. glabra*, a morphologically delimited taxon, was not isolated at first in STRUCTURE. This could be attributable to the clustering algorithms being influenced by unbalanced sampling sizes, masking clade Ko, which appeared isolated at $K = 6$. From $K = 4$ to $K = 6$, the new groups appeared mainly inside the WD clade, showing that the samples from Europe were much more diverse than those from North America. Indeed, the NA clade was not split into subgroups even at $K = 10$. Apart from *B. glabra*, no other named morphospecies formed an exclusive cluster even at high K values.

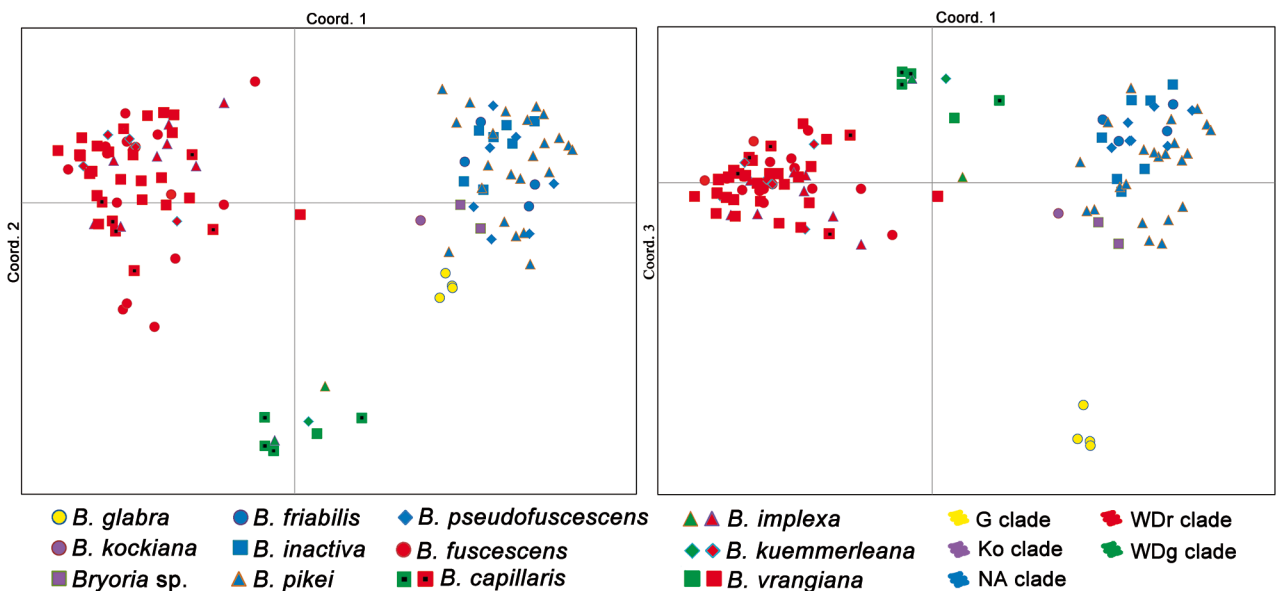


Fig. 3 Principal Coordinate Analysis (PCoA) of microsatellite data in *Bryoria* sect. *Implexae*. Species names according to Velmala et al. 2014 (shape and colours) and STRUCTURE clusters (colours) for each specimen are represented in the three main coordinates. Note that the Ko clade does not appear isolated from the NA clade in any coordinate axis. — G = Glabra clade; Ko = Kockiana clade; NA = North American clade; WD r = Widely Distributed red clade; WD g = Widely Distributed green clade.

Table 3 Species delimitation analysis results for loci ITS, IGS, *GAPDH* and the concatenated data matrix in *Bryoria* sect. *Implexae*. Brackets indicate groups predicted as conspecific. — G = Glabra clade; Ko = Kockiana clade; NA = North American clade; WD = Wide Distributed clade; WD r = Wide Distributed red clade; WD g = Wide Distributed green clade; pik5 = Specimen *Bryoria pikei* 5.

Method	ITS	IGS	<i>GAPDH</i>	Concatenated
ABGD	2 = G + (Ko, NA, WD)	2 = G + (Ko, NA, WD)	4 = G + Ko + NA + WD	4 = G + Ko + NA + WD
PTP	2 = G + (Ko, NA, WD)	2 = G + (Ko, NA, WD)	4 = G + Ko + NA + WD	5 = G + Ko + NA + WD r + WD g
GMYCs	4 = G + (Ko, NA, WD g) + WD r + WD r	3 = G + (Ko, WD) + NA	4 = G + Ko + NA + WD	6 = G + Ko + NA + pik5 + WD r + WD g
GMYCm	4 = G + (Ko, NA, WD g) + WD r + WD r	4 = G + (Ko, WD) + NA1 + NA2	4 = G + Ko + NA + WD	5 = G + Ko + NA + WD r + WD g
DISSECT	–	–	–	5 = G + Ko + NA + pik5 + WD

Principal coordinates analysis (PCoA)

The PCoA analysis has a three-dimensional output represented here in two graphs, one comparing axis 1 against 2, and the other 1 against 3 (Fig. 3). The information percentage of each axis was 44.47 %, 15.06 %, and 14.44 %, respectively. Clade G (Fig. 3, yellow) appeared isolated, whereas clade Ko (Fig. 3, magenta) was admixed with NA clade (Fig. 3, blue), forming a single cluster. Clade WD was isolated from the others, but divided into two clusters, one corresponding to the red and brown groups in the $K = 6$ STRUCTURE output (Fig. 2), and one for the green group. Apart from *B. glabra*, none of the currently accepted morphospecies formed a defined group. Four reasonably isolated clusters could be distinguished, corresponding to the groups G, WDr (Widely Distributed, Fig. 3, red), WDg (Widely Distributed, Fig. 3, green), and Ko together with NA forming a single cluster.

Haplotype network

The haplotype network of the concatenated data matrix, coding gaps as missing data, produced 39 haplotypes. *Bryoria glabra* specimens (Appendix 4, yellow) formed two haplotypes not connected with other members of the network, indicating genetic isolation of this species. One of the haplotypes was composed exclusively of South American specimens, whereas the other contained European, North American, and South American samples. Clade Ko (Appendix 4, magenta) fell into two haplotypes, one including specimens with psoromic acid and identified as *B. kockiana*, and the other clustering unidentified samples with no substances detected. This group was connected to the NA clade (Appendix 4, blue) by a long branch with 13 mutation steps. The NA clade was separated by nine mutations from the WD clade (Appendix 4, green, red, and brown). The WD green, red, and brown groups split by STRUCTURE (Fig. 2) formed a unique cluster. Four isolated clusters could be distinguished, corresponding to the groups G, Ko, NA, and WD.

Species delimitation programs

The ABGD, PTP, GMYC, and DISSECT programs (Table 3) use different algorithms, and consequently different numbers of putative species may be predicted. The genetic distance method (ABGD) gave the smallest number of putative species,

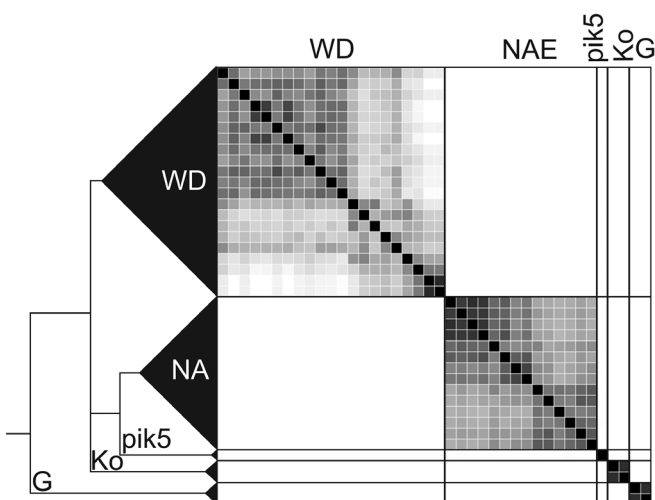


Fig. 4 Similarity matrix from DISSECT analysis performed after clone correction in *Bryoria* sect. *Implexae*. Squares represent posterior probability (white = 0, black = 1) of pairs of specimens to belong to the same species. Resulting major groups are delimited by lines, which indicate the clade on the collapsed phylogenetic tree.

whereas the coalescence methods (especially GMYC) the largest. Analyses also revealed the contribution of each locus to the postulated species delimitation, *GAPDH* being the most informative and constant marker. DISSECT analysis (Fig. 4) predicted five species corresponding to G, Ko, NA, and WD clades, and specimen *B. pikei* 5. Although the GMYC analysis also showed the *B. pikei* 5 specimen as a separate species, it was grouped in the NA clade in the other analyses. DISSECT showed two internal greyish square groups in WD, but they did not correspond exactly to the WDr and WDg groups in Fig. 2, 3 (STRUCTURE and PCoA analyses).

Node dates and demographic history

The calibrated maximum clade credibility chronogram for the concatenated data matrix is shown in Fig. 6. As only the ITS mutation rate is estimated in previous studies (Leavitt et al. 2012a, b), a second chronogram was prepared using this locus alone. Results from this analysis have to be treated with caution, as the species tree is not strictly clock-like (*B. glabra* has a shorter branch), and the ITS mutation rate has been taken from *Melanohalea*, a lichen-forming genus in the same family. Both analyses produced similar values, and the divergence of the *B. glabra* lineage was estimated at 6.9 Mya (95 % HPD = 3.5–10.8) in the concatenated matrix analysis, and 6.5 Mya (95 % HPD = 2.2–11.4) in the ITS data alone. The Ko, NA, and WD split was estimated at 1.0 Mya (95 % HPD = 0.3–2.2) from the concatenated matrix and 0.6 Mya (95 % HPD = 0.2–1.5) from the ITS data alone.

Bayesian Skyline Plots (Fig. 5, left) indicate a recent population increase in the NA and WD clades. However, the sequences contained few informative mutations and the deepest coalescence was reached in around 700 000 yr, with no population changes detectable further back from this period. Tests of neutrality (Fig. 5, right) are commonly used to support inferences from Bayesian Skyline Plots. As indicated by non-significant Tajima's D and F_s results, all sampled groups seem in mutation-drift equilibrium, with the exception of the *GAPDH* locus of the NA clade which had a significant negative D value (Fig. 5 **bold**). This could indicate a recent expansion or 'purifying' selection, as seen in the concatenated Bayesian Skyline analysis, but other loci did not support this hypothesis.

Markers ITS, IGS, and *GAPDH* indicate population stability over the recent past for clades NA and WD, with putative even more recent small population expansions. Due to the low variability of the loci, and the putative loss of demographic signals, this hypothesis is not confirmed by this analysis.

Integrated assessment of datasets

Depending on the analysis, different numbers of putative species were suggested, ranging from four to six (Table 4). All analyses, however, confirmed that the combination of morphological and chemical characters generally used for species circumscription in the complex was inadequate. *GAPDH*, despite its low variability, was the only marker tested that supported species-rank assignments for the clades G, Ko, NA, and WD (Table 3). ITS, one of the most used loci for DNA barcoding in lichen-forming fungi, did not unambiguously distinguish those clades. The new markers FRBi15 and FRBi16, despite their higher variability, showed inconclusive results and putative recombination events. The microsatellite data (Fig. 2) supported the DNA sequences results and reflected internal variability not revealed in our sequence data, showing that the WD cluster was much more diverse than NA, which had a particularly low diversity.

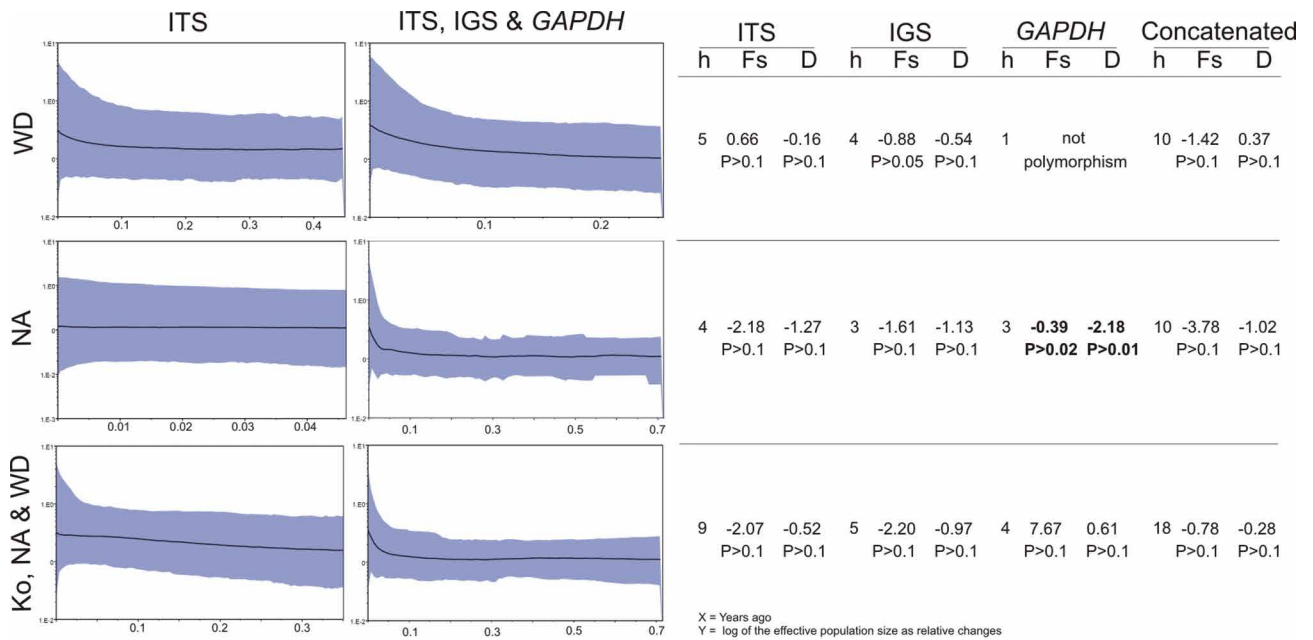


Fig. 5 *Bryoria* sect. *Implexae*. – Left. Bayesian Skyline Plots for each clade predicted by the ITS marker and the concatenated loci matrix. The X-axis of each graph represent time (in Myr), and the Y-axis represents the value for the log of the effective population size as relative changes, because generation times in *Bryoria* species are unknown. Grey shadows indicate the upper and lower 95 % credible intervals. – Right. Results from neutrality tests for each marker and clade, indicating (in **bold**) any statistically significant deviation from neutrality. — h = number of haplotypes; Fs = Fu's Fs; D = Tajima's D.

Table 4 Summary of the number of putative species suggested by the different methods used for each dataset in *Bryoria* sect. *Implexae*.

Method	Data	Figure / reference	Number of putative species
Traditional concept	DNA sequences and phenotypic	Velmala et al. (2014)	12
Chemical	Phenotypic	Appendix 2 Left	c. 4
Morpho-chemical	Phenotypic	Appendix 2 Right	Not conclusive
Phylogeny	DNA sequences of ITS, IGS, and <i>GAPDH</i>	Fig. 6	4 = G + Ko + NA + WD
Phylogeny	DNA sequences of FRBi15	Fig. 1	Not conclusive
Phylogeny	DNA sequences of FRBi16	Fig. 1	Not conclusive
STRUCTURE	Microsatellites	Fig. 2	5 = G + Ko + NA + WDr + WDg
PCoA	Microsatellites	Fig. 3	4 = G + (Ko, NA) + WDr + WDg
Haplotype Network	DNA sequences of ITS, IGS, and <i>GAPDH</i>	Appendix 4	4 = G + Ko + NA + WD
ABGD	DNA sequences of ITS, IGS, and <i>GAPDH</i>	Table 3	4 = G + Ko + NA + WD
PTP	DNA sequences of ITS, IGS, and <i>GAPDH</i>	Table 3	5 = G + Ko + NA + WDr + WDg
GMVCs	DNA sequences of ITS, IGS, and <i>GAPDH</i>	Table 3	6 = G + Ko + NA + pik5 + WDr + WDg
GMVCm	DNA sequences of ITS, IGS, and <i>GAPDH</i>	Table 3	5 = G + Ko + NA + WDr + WDg
DISSECT	DNA sequences of ITS, IGS, and <i>GAPDH</i>	Fig. 4	5 = G + Ko + NA + pik5 + WD

TAXONOMY

Bryoria* sect. *Implexae (Gyeln.) Brodo & D. Hawksw., Opera Bot. 42: 114. 1977

Basionym. *Bryopogon* sect. *Implexae* Gyeln., Feddes Repert. Spec. Nov. Regni Veg. 38: 223, 238. 1935.

Type species. *Bryoria implexa* (Hoffm.) Brodo & D. Hawksw. 1977. ≡ *Usnea* [unranked] *implexa* Hoffm. 1796. = *Bryoria fuscescens* (Gyeln.) Brodo & D. Hawksw. 1977; but see below.

Species with a fruticose, hair-like, subpendent to mainly pendent thallus, lateral spinules or spinulose branches absent, whitish grey to brown or black, often paler in the basal parts. Angles between branches variable, acute to obtuse or even rounded. Pseudocyphellae absent or present, then frequently inconspicuous, ± fusiform, concolorous or whitish. Soralia ab-

sent or present, tuberculate or fissural, white to dark. Isidia or isidioid spinules absent. Apothecia mainly absent, if present, usually afunctional. Chemistry varied, with no detectable or with one or a combination of major substances, including alectorialic, barbatolic, connorstictic, fumarprotocetraric, gyrophoric, norstictic, protocetraric, psoromic and possibly salazinic acids, atranorin, and chloroatranorin. Photobiont *Trebouxia 'hypogymniae'* (Lindgren et al. 2014).

Notes — Most species included in Brodo & Hawksworth (1977) under *Bryoria* sect. *Implexae* were transferred to other sections in Myllys et al. (2011). In the light of our results (but see the Discussion later), *Bryoria* sect. *Implexae* includes the four species treated below. Comments on particular morphological or chemical traits that may be helpful for distinguishing these taxa are given under each species. Nevertheless, nearly all cited characters are shared by different taxa, so they can

be interpreted as 'cryptic'. The species names adopted here are epitypified by sequenced material here in order to fix their identities at the molecular level. This epitypification is essential to fix the application of these names as no DNA sequences are available and cannot be obtained from old type material of most species names. The old types cannot therefore be critically identified for purposes of the precise application of the names and so epitypes may be designated (Turland et al. 2018: Art. 9.9 and Ex 9).

As molecular data are necessary for unambiguous species level identification in the taxonomy proposed here, we recommend using the collective '*Bryoria fuscescens* complex' when referring to material lacking molecular data.

Bryoria fuscescens (Gyeln.) Brodo & D. Hawksw., *Opera Bot.* 42: 83. 1977

Basionym. *Alectoria fuscescens* Gyeln., *Nytt Mag. Naturvidensk.* 70: 55. 1932, nom. cons. (cf. Hawksworth & Jørgensen 2013).

Synonyms. *Lichen chalybeiformis* L., *Sp. Pl.* 2: 1155. 1753, (nom. cons.) nom. rej. against *Bryoria fuscescens* (cf. Hawksworth & Jørgensen 2013).

Bryoria chalybeiformis (L.) Brodo & D. Hawksw., *Opera Bot.* 42: 81. 1977.
Usnea [unranked] *implexa* Hoffm., *Deutschl. Fl., Zweiter Teil.* 134. 1796.
Bryoria implexa (Hoffm.) Brodo & D. Hawksw., *Opera Bot.* 42: 121. 1977.
Parmelia jubata β. [var.] *capillaris* Ach., *Methodus, Sectio post.*: 273. 1803.

Bryoria capillaris (Ach.) Brodo & D. Hawksw., *Opera Bot.* 42: 115. 1977.
Alectoria jubata ζ. [var.] *lanestris* Ach., *Lichenogr. Universalis*: 593. 1810.
Bryoria lanestris (Ach.) Brodo & D. Hawksw., *Opera Bot.* 42: 88. 1977.
Alectoria kuemmerleana Gyeln., *Nytt Mag. Naturvidensk.* 70: 49. 1932.
Bryoria kuemmerleana (Gyeln.) Brodo & D. Hawksw., *Opera Bot.* 42: 155. 1977.

Alectoria proluxa var. *subcana* Nyl. ex Stizenb., *Ann. Naturhist. Mus. Wien* 7: 129. 1892, nom. rej. against *Bryoria fuscescens* (cf. Hawksworth & Jørgensen 2013).

Bryoria subcana (Nyl. ex Stizenb.) Brodo & D. Hawksw., *Opera Bot.* 42: 91. 1977.

Alectoria vrangiana Gyeln., *Magyar Bot. Lapok* 31: 46. 1932.

Bryoria vrangiana (Gyeln.) Brodo & D. Hawksw., *Opera Bot.* 42: 97. 1977.

Type specimens. FINLAND, Tavastia austr., Hollola, ad truncos *Pini* locis apricioribus in silva, Sept. 1882, J.P. Norrlin (Norrlin, *Herb. Lich. Fenn.* No. 46) (BP 33947 – lectotype designated by Hawksworth 1972: 217). — FINLAND, Etelä-Savo, Savitaipale, 600 m NW of Mustapää, 61, N1721° E27,6900°, 2005, L. Myllys 464 (HA.H9209715 (L139)) – epitype designated here, MycoBank MBT381730.

Nomenclature — A large number of species rank names belong to this group, and are synonymised, but these have not been epitypified with sequenced material. Further information on synonyms and type materials can be seen in Hawksworth (1972), Brodo & Hawksworth (1977) and Velmala et al. (2014). Although no samples of *Bryoria austromontana* have been studied, the published description and images (Jørgensen & Galloway 1983) suggest this taxon also belong here.

The earliest species rank epithets amongst these are *chalybeiformis* dating from 1753 (*Lichen chalybeiformis*), and *implexa* dating from 1799 (*Usnea implexa*). The former has been rejected against *Bryoria fuscescens*, but not against other species names apart from *B. subcana* (Hawksworth & Jørgensen 2013). A proposal to add the four earlier names *Alectoria capillaris*, *Usnea implexa*, *A. kuemmerleana*, and *A. lanestris* to the two against which *Alectoria fuscescens* is already conserved is being prepared separately. Protection against *A. vrangiana* is not required as it appeared in the same work as *A. fuscescens*. While the proposal is under discussion, the name *B. fuscescens* should be adopted in accordance with Rec. 14A.1 (Turland et al. 2018).

We refrained from epitypifying and taking up any of the earlier and potentially competing names by epitypification primarily as the name *B. fuscescens* is the most commonly used species

name in the complex, is well established, the most widely used* and is already conserved over two earlier species names in the complex. In addition, all the other names have been associated with particular morphotypes or chemotypes since the 1970s, and so their use might be mistaken as applying to a taxon with those particular traits.

If the proposal for rejection of the previously mentioned competing synonyms is not accepted, the principle of priority would rule the use of the earliest and not already rejected, validly published name at the species rank, i.e., *Usnea implexa* (and then the combination *Bryoria implexa*), which would require epitypification by sequenced material in order to fix the precise application of that name. The species was first described from Germany but with no named locality, and neotypified by an unlocalised and undated specimen in Hoffmann's herbarium in Moscow (*Hoffmann 8569*, MW) which may be part of the original material from Germany or have been collected later and perhaps in Russia (Hawksworth 1969a). As the neotype contained psoromic acid, and the epithet has therefore been applied to that chemotype, a potential sequenced epitype should represent that chemotype and ideally also have been collected in Germany. No such specimen was available to us during this study.

Distribution — Widely distributed, known from cool temperate to boreal and arctic areas of Europe, Asia, North America, and Africa. There are also reports from Antarctica, Oceania, and South America, but material from those regions has not yet been studied molecularly and so we cannot confirm that they belong to this complex.

Notes — *Bryoria fuscescens* is highly variable in morphology and chemistry, and many of the analysed specimens develop soralia. Further, atranorin, which is not normally detectable in the other three species accepted here, is frequently found in concentrated extracts from both sorediate and esorediate morphs.

Bryoria glabra (Motyka) Brodo & D. Hawksw., *Opera Bot.* 42: 86. 1977

Basionym. *Alectoria glabra* Motyka, *Fragm. Florist. Geobot.* 6: 448. 1960.

Type specimens. USA, Washington, Olympic Peninsula, Clallam Co., Hurricane Ridge, 5800 ft, on trunk of *Abies lasiocarpa*, 24 July 1950, B.I. Brown & W.C. Muenscher 129 (US – holotype). — USA, Alaska, Mainland, Valley between the Bucher and Gilkey Glaciers, southern end of subalpine valley, on east side of creek running through valley, subalpine forest, N58°47'20.12" W134°30'0.10", 773 m elevation, on *Tsuga mertensiana* twigs, 4 Aug. 2011, K.L. Dillman 4Aug11:1 (UBC (L406)) – epitype designated here, MycoBank MBT381731.

Distribution — Known from northern Europe (Scandinavia), and North and South America. In North America, it is most abundant in the Pacific North-West.

Notes — Distinguishing features in well-developed specimens are the brownish thallus with a regular branching pattern, generally with obtuse and rounded angles between the branches, and broad oval and usually white soralia. It is, however, difficult to separate poorly developed or small specimens conclusively, so molecular sequences are recommended for unambiguous identifications. Only fumarprotocetraric and protocetraric acids have been detected in this species, and these are characteristically produced in the soralia.

The Alaskan specimen is selected as the epitype here as sequences are available from all loci, whereas the material we

* Hits obtained for these names in Google and Google Scholar respectively on 12 April 2018 were: *B. fuscescens* (12300 and 1620), *B. capillaris* (10300 and 999), *B. implexa* (6020 and 447), *B. kuemmerleana* (226 and 20), *B. lanestris* (6740 and 185), and *B. vrangiana* (532 and 61).

have sequenced from Washington state (type locality) only has data on the ITS locus.

Bryoria kockiana Velmala, Myllys & Goward in Velmala et al., *Ann. Bot. Fenn.* 51: 361. 2014

Type specimen. USA, Alaska, Fairbanks, North Star Borough, 26 July 2011, *D. Nossov 20019-1* (UBC (L394) – holotype).

Distribution — Known only from Alaska (USA) and British Columbia (Canada), on conifer branches.

Notes — Few specimens of this species have so far been studied, and these are characterised by the absence of any whitish grey tone in the thallus, the lack of soralia, and greyish to brown branches with conspicuous, white to concolourous, broad, elongate-fusiform, sometimes slightly raised pseudocyphellae. It lacks TLC-detectable substances or produces psoromic acid. The not validly published designation *Alectoria krogii* D. Hawksw. 1972 may be synonymised here.

Bryoria pseudofuscescens (Gyeln.) Brodo & D. Hawksw., *Opera Bot.* 42: 127. 1977

Basionym. *Alectoria pseudofuscescens* Gyeln., *Ann. Hist.-Nat. Mus. Natl. Hung.* 28: 283. 1934, and *Rev. Bryol. Lichénol.* 7: 51. 1934.

Synonyms. *Bryoria friabilis* Brodo & D. Hawksw., *Opera Bot* 42: 118. 1977.

Bryoria pikei Brodo & D. Hawksw., *Opera Bot* 42: 125. 1977.

Bryoria inactiva Goward et al., *Ann. Bot. Fenn.* 51: 360. 2014.

Type specimens. USA, Oregon, Benton County, Corvallis, on old apple trees, Dec. 1931, *F.P. Sipe* 669 (BP 33958 – holotype of *Alectoria pseudofuscescens*). — CANADA, British Columbia, 25 Sept. 2006, *T. Goward 07-02-2011* (UBC (S222) – epitype selected here, MycoBank MBT381732; British Columbia, Clearwater Valley, 0.5 km S of Philip Creek, 'Edgewood West', 715 m, 9 Nov. 2011, *T. Goward 11-61* (UBC (L347) – holotype of *Bryoria inactiva*).

Nomenclature — A number of species rank names are synonymised to this taxon, but these have not been epitypified with sequenced material. All these names, however, are later in date than *pseudofuscescens*, and so could not have priority over that name. Further information on type materials can be seen in Brodo & Hawksworth (1977) and Velmala et al. (2014). Although no samples of *Bryoria salazinica* have been studied at molecular level, the published description and images (Brodo & Hawksworth 1977) suggests this taxon also belong here.

Distribution — Only known from North America, growing on bark, branches, rock or soil.

Notes — Characterised by the absence of soralia and detectable atranorin.

DISCUSSION

Phylogenetic relationships

Species concepts in *Bryoria* sect. *Implexae* have previously been based primarily on well-characterised northern European and North American specimens (Hawksworth 1972, Brodo & Hawksworth 1977, Velmala et al. 2014). Velmala et al. (2014) recognised 11 species on the basis of morphological and chemical characters, but many of these were not supported by molecular data, and different species names were accepted for taxa that could not be distinguished molecularly. We discovered that these demarcations broke down when specimens from more southern European populations were incorporated. This is shown in a phenetic analysis using only phenotypically diagnostic characters (Appendix 2), where the resulting groups are not resolved as clear-cut morphospecies. Indeed, any character previously used in the group could be used to define the three lineages of the *Bryoria fuscescens* complex (Fig. 6).

Sexual structures are of major importance in species identification in fungi, but here the rarity of apothecial production has hampered their study in most *Bryoria* species. Any such features found would in any case be of limited practical value in identification as nearly all samples lack apothecia. Extrolite composition has been accorded a major role in species delimitation in the complex, but many of the substances that were considered to be of diagnostic value are biosynthetically closely related, being produced by the same gene cluster (pks genes; Keller & Hohn 1997), and may be environmentally influenced (Myllys et al. 2016, Lutsak et al. 2017).

Integrative taxonomy, rather than phylogenies based only on neutral markers, are increasingly being used to resolve complex taxonomical groups (e.g., Dayrat 2005, Will et al. 2005, Lumley & Sperling 2011, Zamora et al. 2015, Caparrós et al. 2016). Microsatellites are also now widely used in intraspecific population studies because of their high variability (Widmer et al. 2012, Dal Grande et al. 2014), and in species complexes with diffuse genetic barriers, microsatellite data can improve DNA sequence resolution (Lumley & Sperling 2011, Vanhaecke et al. 2012). It is generally assumed that DNA sequence data reflect the evolution of the species, but these data only reflect the history of the studied loci, which may sometimes be different from the species history overall (Nichols 2001). In this case, we demonstrated that traditionally used loci (ITS, IGS, and *GAPDH*) and microsatellite data reveal similar clades, whereas other intergenic loci (FRBi15 and FRBi16) produced discrepant but statistically supported lineages. These incongruences may be due to recombination, hybridisation, or incomplete lineage sorting, as documented in many other species groups (e.g., Jakob & Blattner 2006, McGuire et al. 2007, Edwards et al. 2008, Stewart et al. 2014). In lichen-forming fungi, outcrossing and recombination have been demonstrated, for example, in *Lobaria pulmonaria* (Zoller et al. 1999, Singh et al. 2012, Keller & Scheidegger 2016), *Letharia* (Kroken & Taylor 2001a, b, Altermann et al. 2014), and *Cladonia* (Steinová et al. 2013).

Apothecia are usually absent in *Bryoria* sect. *Implexae*, and even when present may not contain mature spores. If cryptic sexuality is not occurring, hybridization is unlikely to provide an explanation of our data. In the absence of sexual reproduction, any recombination is improbable, although some fungi lacking sexual structures show recombination events attributable to parasexual cycles (Schoustra et al. 2007). We did detect signals suggesting putative recombination in the FRBi loci, but not in the standard three loci used in the taxonomy adopted here. Recombination signals may reflect some mitotic recombination, actual or ancient sexual reproduction (Douhan et al. 2007) or be merely false positives produced by chance production of similar sequences. In any case, recombination alone is insufficient to explain all the discordances found. For example, only one putative recombination event was detected in FRBi15, and disentangling the FRBi16 recombination points is insufficient to obtain the topology of the three-locus phylogeny. Incongruences may also be caused by the analysis of different paralogs of FRBi15 and FRBi16 amplified with the new primers, but this seems improbable, as no paralogs have been detected in the SSRs of these loci (Boluda et al. unpubl.). However, our results indicate recent diversification and large effective population sizes in this lichenised complex. Thus, incongruences amongst loci seem rather attributable to incomplete lineage sorting.

The different putative species concepts generated by the species delimitation programs (Table 3) may not be only due to the different algorithms applied, but also because some of the programs were designed for use in single-locus phylogenies (e.g., ABGD, PTP, or GMYC). Nevertheless, all the clustering analyses showed a tendency to distinguish four groups, G, Ko, NA, and WD (Table 4; Fig. 6). STRUCTURE was unable to

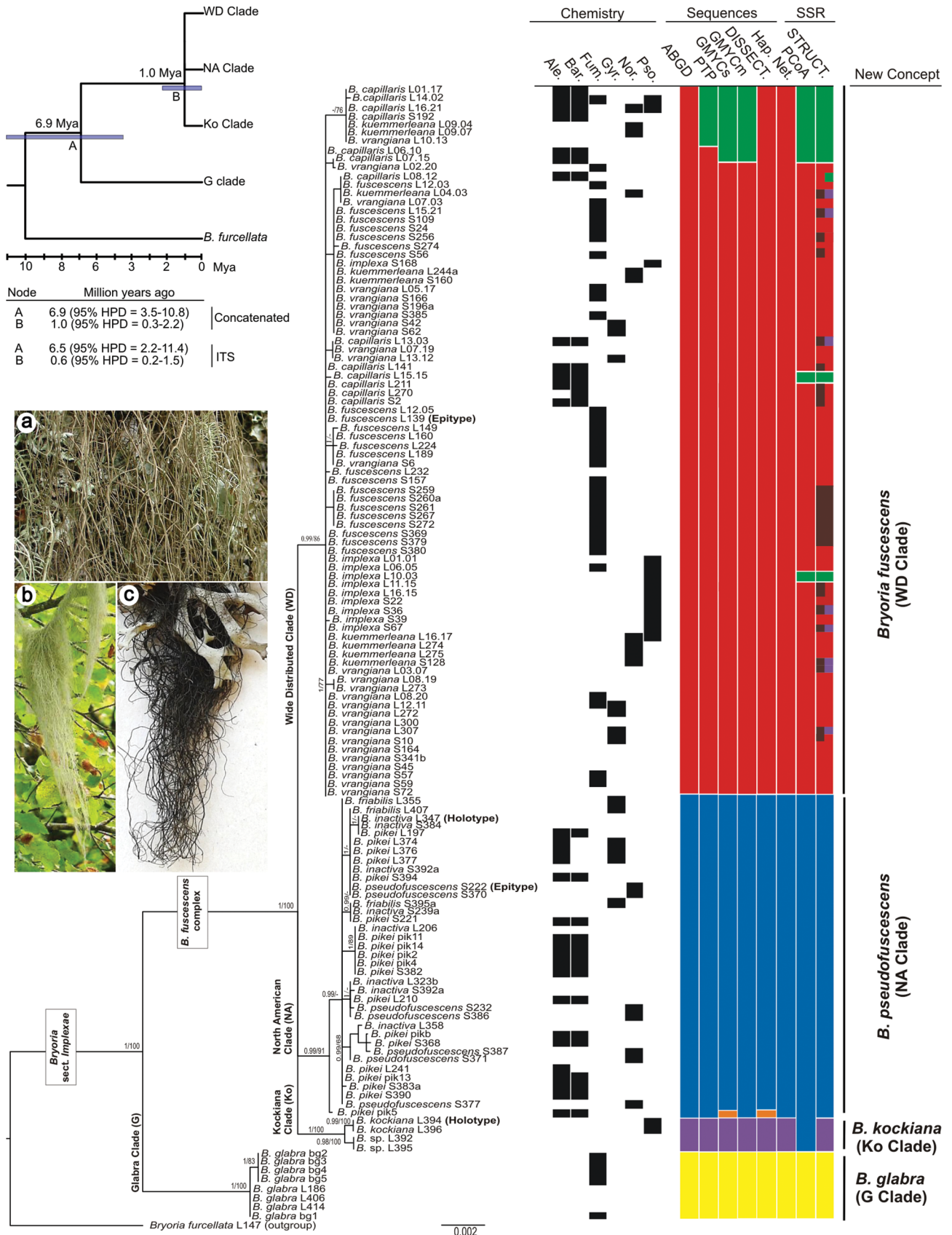


Fig. 6 Integrated assessment of results in *Bryoria* sect. *Implexae*. Tree topology depicts the result of the Bayesian Markov chain Monte Carlo (B/MCMC) analysis. Posterior probabilities and bootstrap analysis for the supported nodes (≥ 0.95 and $\geq 70\%$) are indicated at the main nodes. For each specimen, the extrolites detected, and the putative number of species predicted by the different methodologies is shown. The left top corner tree shows the results of the molecular dating analysis. — a. *Bryoria implexa* morphotype (Spain, Asturias, 2013, Boluda, MAF-Lich. 20749); b. *B. capillaris* morphotype (Spain, Navarra, 2013, Boluda & Villagra, MAF-Lich. 20748); c. *B. fuscescens* morphotype (Morocco, Ifrane, 2013, Boluda, MAF-Lich. 20751). — Ale. = Aleoctorial acid; Bar. = Barbatolic acid; Fum. = Fumarprotocetraric acid; G = Glabra clade; Gyr. = Gyrophoric acid; Hap. Net. = Haplotypic Network; HPD = Highest Posterior Density; Ko = Kockiana clade; Mya = Million years ago; NA = North American clade; Nor. = Norstictic acid; PCoA = Principal Coordinates Analysis; Pso. = Pso-romic acid; STRUCT. = Structure; WD = Wide Distributed clade.

define these groups until reaching the $K = 6$ hypothesis, which can be attributed to the highly unbalanced sampling sizes; the analyses shows that the WD cluster is much more variable than NA, which was not divided into subgroups until $K = 10$.

Specimen 49 (identified as *B. pikei*, Fig. 2 asterisk), probably reflects the impossibility of unequivocally distinguishing that species from *B. capillaris*; however, as sequence amplification of this specimen failed, we cannot determine if this mismatch was due to misidentification or DNA contamination. Haplotype network analyses have been extensively used in infraspecific population and less frequently closely related species groups (Houbraken et al. 2012, Pino-Bodas et al. 2016). Even this type of nested clade phylogeographic analysis has some critics (e.g., Knowles 2008, Templeton 2009). The resulting network in the present case is concordant with that obtained from other analyses. If two DNA barcoding standard marker networks are obtained from a single analysis with a 95 % parsimony connection limit, members of each network might be considered as different species (Hart & Sunday 2007), showing the clear isolation of *B. glabra* from the other taxa in the complex. In the case of connections with several mutation steps, as between clades Ko, NA, and WD, taxon delimitation is below the species level, but in any case indicates some degree of genetic isolation.

The relationships amongst the Ko, NA, and WD clades remains unresolved, indicating that the evolutionary history may be too complex to be adequately captured by dichotomous phylogenies based on a few neutral markers. Moreover, the putative presence of shared ancestral polymorphisms amongst the clades may be producing incompatible topologies, which result in clades with low support.

We also performed analyses to estimate changes in past population sizes, which may have affected current clade diversity. Genealogies of most plant and animal species coalesce between 2.58–0.01 Mya (Grant 2015), and our estimated intervals are within this range. However, in our case the dates are relatively recent, with the oldest coalescences at 0.7 Mya. A flat graphic is generally interpreted as population stability but can also be due to a lack of detection power produced by small sample sizes. Moreover, a small rise in the curve near the present, seen in Fig. 5, can be a consequence of the random sampling of the MCMC haplotype trees (Grant 2015); this result must therefore be treated with caution. Our sequences do not bear imprints of ancient population history, but rather more recent population growth, for example by extensions northwards in post-glacial periods. The loss of information may also arise from bottlenecks (i.e., a marked reduction in population size), local extinctions, and subsequent recolonization. Additionally, the use of genes with low levels of polymorphisms, may impede a robust reconstruction of population sizes through time.

Species concept

Some species delimitation analyses, such as STRUCTURE, GMYC, PTP, can overestimate the number of taxa meriting formal recognition, particularly when sampling is uneven or in species with a strong intraspecific genetic structure (Altermann et al. 2014, Modica et al. 2014, Alors et al. 2016, Del-Prado et al. 2016). ABGD, in contrast, has been considered as rather conservative, less prone to species overestimation and less sensitive to unbalanced sampling. While that method only detects discontinuities in DNA sequence variation (Puillandre et al. 2011), it can also be expected to fail in species with strong population genetics structures, for example ones containing exclusive haplotypes. All species delimitation programs will provide a number of reasonably discrete groups ('evolving lineages') that should be evaluated for consideration as meriting species rank, but the decision has to be by taxonomists with experience in the group concerned. Some of our analyses

suggest that groups such as WDr, WDg, or pik5 might merit species rank, but our experience, together with the results from other analyses shown here, leads us to reject this hypothesis. We conclude that the most pragmatic solution, supported by the general trend of the results from the different analyses we performed is to consider clades G, Ko, NA, and WD as the species *Bryoria glabra*, *B. kockiana*, *B. pseudofuscescens*, and *B. fuscescens*, respectively.

Clade age can contribute to decisions as to species limits. Divergence time estimates can be robust if the analyses are performed with well-resolved phylogenies and can incorporate fossil calibration points, as in some vertebrates (Perelman et al. 2011). Contrarily, in lichenised fungi, fossils are rare and in many cases enigmatic or with ambiguous relationships (Thomas et al. 2014, Hawksworth 2015, Kaasalainen et al. 2015). In addition, generation times can be expected to be different among species, as is the case with nuITS locus mutation rates between herbaceous and woody plants, or even a difference of almost an order of magnitude between different plant genera (Kay et al. 2006). Here we used a nuITS mutation rate estimated from *Melanohalea*, a genus in the same family (Leavitt et al. 2012a), species of which frequently grow with *Bryoria* and reproduce asexually as well as sexually. The split of *B. glabra* from the other taxa in the *B. fuscescens* complex is estimated at c. 6.9 Mya, and clearly separated from the much later divergence of the other three species estimated at c. 1 Mya (0.6 Mya if only the nuITS locus is used). This contrasts with other lichenised species considered of recent origin, estimated around 2.5–5 Mya (Pliocene), with any Pleistocene speciation event rare and always older than 1 Mya (Amo de Paz et al. 2012, Leavitt et al. 2012a, b, Molina et al. 2016). As the three *B. fuscescens* complex clades seem to have diverged more recently, the extent of their reproductive isolation is uncertain, and the discovery of intermediate lineages amongst other named species from unsampled geographical regions, such as continental Asia remains possible.

In the absence of supporting phenotypic, geographic, or ecological differences, the recent divergence, and the possibility of incomplete lineage sorting, clades Ko, NA, and WD may be considered as conspecific evolving lineages. It is, however, important to recognise the lineages formally in order to facilitate their conservation by enabling their threat status to be assessed by IUCN criteria. We decided not to adopt the rank of subspecies as that is now hardly used in mycology, and then not in any consistent way; traditionally this rank was used in plants for morphologically distinguishable populations with geographical differences and where intermediates occurred where they were sympatric (Stuessy 2009).

The formal recognition of cryptic lineages at species level, as suggested by our analyses, emerges as the most appropriate solution. Cryptic speciation is now recognised as a common phenomenon in *Parmeliaceae*, and our results are in accord with other studies in which molecular markers in combination with statistical tools revealed genetically distinct lineages previously hidden under a single taxon name in this family (e.g., Singh et al. 2015, Alors et al. 2016, Del-Prado et al. 2016, Divakar et al. 2016, Leavitt et al. 2016). Further, this solution is in line with the increasing need to formally recognize cryptic species-level lineages in all fungi (Hibbett 2016); indeed, cryptic speciation may mean that there are on average ten or more fungi masked in formally named species (Hawksworth & Lücking 2017).

Of the lineages recognised here, only the WD clade emerged as cosmopolitan, occurring in Europe, Asia, North America, and Africa (Appendix 5). NA and Ko have been collected so far only in North America, despite our extensive sampling in Europe

(Appendix 5). Further sampling, especially in South America, Asia, and Africa, is needed before any finer-scale biogeographic patterns might be detected.

The practical issue of naming older museum specimens and material in ecological surveys could be resolved by recognising the three groups as species within a broad concept, such as an aggregate, complex, or adding 's.lat.'. We considered commending the adoption of the suffix 'agg.' for material when precise molecular species identifications cannot be made. While this has been done in a few other groups of fungi (e.g., Parnmen et al. 2013, Pažoutová et al. 2015), 'complex' has come to be used more widely and was strongly favoured at the Cryptic Speciation in Fungi symposium in Utrecht in September 2017 (report awaited). We therefore suggest the use of 'complex' here but recognise some may prefer to use 'agg.' or 's.lat.'. Where DNA samples can be obtained and analysed, we recommend use of the *GAPDH* locus, as all the other tested markers are not able to distinguish with confidence the three species we recognize in the complex.

Intraspecific phenotypic variation

While our results support rejection of the morphospecies concept in this group of lichens, two main phenotypes can nevertheless often be distinguished by the naked eye in the field:

1. the pale grey '*capillaris*' morphotype (including *B. capillaris* and *B. pikei*, Fig. 6b); and
2. the fuscous brown to dark brown '*fuscescens*' morphotype, in which most other species names are placed (Fig. 6a, c).

The chemical characters are not always checked by field workers, and while the '*capillaris*' morphotype typically has benzyldepsides, the '*fuscescens*' morphotype lacks those compounds and has fumarprotocetraric acid or various depsidones. However, there are dark morphs with benzyldepsides (once called f. *fuscidula*), and pale grey ones with fumarprotocetraric acid (e.g., *B. subcana*) or other depsidones (e.g., *B. kuemmerleana*). It is conceivable that the two morphotypes originated before the separation of *B. pseudofuscescens* and *B. fuscescens*, as both colour variants and chemistries appear in both taxa. This phenomenon cannot be explained by a simple ongoing speciation event in which one lineage has originated new adaptations, but is still not isolated from the parental lineages, as neither are monophyletic in a paraphyletic clade.

The difference in phenotype cannot be attributed to different algal partners as all material in the complex shares the same species and even in many cases the same nullTS haplotypes of *Trebouxia* (Lindgren et al. 2014, Boluda et al. unpubl.). Further, as we used neutral markers to detect gene-flow gaps between lineages, the phenotypes are also not the result of genetic isolation, and other possibilities must be considered.

It has recently been reported that yeast morphs of the lichenicolous and gall-forming basidiomycete genus *Cyphobasidium* can be abundant in or on the outermost cortical tissues of *Bryoria* species (Spribille et al. 2016). Spribille et al. (2016) reported a possible relation between *Cyphobasidium* yeast abundance and vulpinic acid production in two other species of *Bryoria*, *B. fremontii* and *B. tortuosa*, and also visualised these yeasts in material identified as *B. capillaris* phenotypes. Contrary to the claims of Spribille et al. (2016), these fungi do not appear to be an integral part of the mutualism (Oberwinkler 2017). It is, however, feasible that the yeasts cells are able to develop to a greater extent in '*capillaris*' morphotypes as the cortices can have lumpier polysaccharide deposits than do those of '*fuscescens*' (Hawksworth 1969b, Boluda et al. 2014, Esseen et al. 2017). How the occurrence of yeast morphs of these lichenicolous fungi in the surface of the cortex could possibly determine colour morphotypes is obscure.

Material referred to the '*capillaris*' and '*fuscescens*' phenotypes has been reported to show slight differences in water holding capacity (Esseen et al. 2015), and also the pigments may provide protection against excesses of light (Färber et al. 2014). Further, in southern Europe particularly, the '*capillaris*' phenotype tends to be restricted to humid, shaded, and protected or undisturbed environments than the '*fuscescens*' one, something already recognised by Motyka (1964). Additionally, in northern Europe, dark specimens containing barbatolic acid are much more common than in southern Europe, where they are extremely rare (Myllys et al. 2016, Esseen et al. 2017). As both phenotypes can grow side by side and even intermixed on the same trees, where environmental conditions must be identical, ecological plasticity has to be discounted. However, some unknown epigenetic modification could perhaps have a role in that process, as once a metabolic pathway is activated or silenced, it may be hardly modifiable under more or less neutral environmental conditions, transferring the phenotypes to the clonal offspring. Specimens with dark thalli, containing barbatolic acid, or with pale thalli with traces of barbatolic and also containing other extrolites, could represent transitional specimens.

Molecular and morphological rates of divergence may sometimes be uncoupled. Incomplete lineage sorting arises when an ancestral polymorphism persists through a speciation event and each polymorphism can lead to different alleles being carried among descendants (Maddison 1997, Hartl & Clark 2007). Consequently, different tree topologies may be obtained depending which specimens or loci are used. Rosenberg (2003) has shown that $5.3N_e$ generations are needed for a species to acquire monophyly at 99 % of its loci given that all loci in the sister species are also monophyletic. That indicates that for a species of 1 M individuals with a generation time of 10 yr, the full monophyly will only be reached 50 M years after speciation, whereas only around 1 000 yr may be needed for species with small populations (Naciri & Linder 2015). Incomplete lineage sorting may be frequent in closely related taxa or during a speciation process (Hobolth et al. 2011, Blanco-Pastor et al. 2012, Saag et al. 2014, Naciri & Linder 2015), as may be considered in our case. The topological incongruence observed among the standard loci, FRBi15 and FRBi16, supports the incomplete lineage sorting hypothesis as one of the main reasons explaining why morphospecies are not monophyletic. While neutral markers are useful for understanding gene-flow patterns, adaptive markers provide the evolutionary pressure that contributes to speciation (Emelianov et al. 2004, Hey 2006, Holderegger et al. 2006). As adaptive markers are under natural selection, certain alleles can be present in some morphospecies and absent in others, even if there is gene flow amongst them (Lumley & Sperling 2011). The use of phylogenomic datasets may provide a more accurate and supported phylogenetic reconstruction, especially if the appropriate scale of loci variability is selected from all the genome (Leavitt et al. 2016). However, if there are high levels of incomplete lineage sorting, it might not be expected that morphospecies would appear forming supported clades. Nevertheless, genomic data may reveal few mutations linked to certain morphospecies, which would be producing adaptive traits. Darwin's finches are an iconic example of a rapid speciation process, in which there is a mismatch between the phylogenetic species concept and phenotype-based taxonomy; in that case, genomic studies have detected specific loci subjected to selection pressure, which are directly related with the development of taxon-specific phenotypes (Lamichhaney et al. 2015). In *Bryoria*, supposed adaptive traits may be influenced by the genes involved in the production of certain extrolites or in the epicortical substances (Boluda et al. 2014), which may produce differential selection pressure for each morphotype,

at least in some environments. The process might be similar to that of natural selection of the pale and melanic morphs of the Peppered Moth (*Biston betularia*) in Europe (Majerus 2009), impeding the fixation of a single morphotype in all populations. In our case also, high levels of incomplete lineage sorting mixed with a few phenotypically important genes under variable degrees of selection in different environments, may explain the mismatch observed between phenotypes and genotypes.

Acknowledgements This work was undertaken with the support of the Spanish Ministerio de Economía y Competitividad projects CGL2011-25003 and CGL2014-55542-P, and the BES-2012-054488 grant to CGB. Microsatellite analyses carried out at WSL were financially supported by the Federal Office for the Environment (FOEN) and SwissBOL (grants to CS), and we acknowledge the Genetic Diversity Centre at ETHZ. We are grateful also to A. Crespo (Madrid), B. Abbott (Arkadias), C. Ruibal (Madrid), H. Holien (Steinkjer), J. Villagra (Madrid), M. Wedin (Stockholm), N. Calpena-Grau (Madrid), and T. Goward (Vancouver) for providing specimens. We are especially grateful to C. Cornejo (Switzerland) for her help with the laboratory work, and for a helpful review of the manuscript.

REFERENCES

- Abbott RJ, Barton NH, Good JM. 2016. Genomics of hybridization and its evolutionary consequences. *Molecular Ecology* 25: 2325–2332.
- Akaike H. 1974. A new look at the statistical model identification. *IEEE Transactions on Automatic Control* 19: 716–723.
- Alors D, Lumbsch TH, Divakar PK, et al. 2016. An integrative approach for understanding diversity in the *Punctelia rudecta* species complex (Parmeliaceae, Ascomycota). *PLoS ONE* 11: e0146537.
- Altermann S, Leavitt SD, Goward T, et al. 2014. How do you solve a problem like *Letharia*? A new look at cryptic species in lichen-forming fungi using Bayesian clustering and SNPs from multilocus sequence data. *PLoS ONE* 9: e97556.
- Amo de Paz G, Cubas P, Crespo A, et al. 2012. Transoceanic dispersal and subsequent diversification on separate continents shaped diversity of the *Xanthoparmelia pulla* group (Ascomycota). *PLoS ONE* 7: e39683.
- Articus K, Mattsson J-E, Tibell L, et al. 2002. Ribosomal DNA and β -tubulin data do not support the separation of the lichens *Usnea florida* and *U. subfloridana* as distinct species. *Mycological Research* 106: 412–418.
- Bekessy SA, Ennos RA, Burgman MA, et al. 2003. Neutral DNA markers fail to detect genetic divergence in an ecologically important trait. *Biological Conservation* 110: 267–275.
- Blanco-Pastor JL, Vargas P, Pfeil BE. 2012. Coalescent simulations reveal hybridization and incomplete lineage sorting in Mediterranean *Linaria*. *PLoS ONE* 7: e39089.
- Boluda CG, Hawksworth DL, Divakar PK, et al. 2016. Microchemical and molecular investigations reveal *Pseudephebe* species as cryptic with an environmentally modified morphology. *The Lichenologist* 48: 527–543.
- Boluda CG, Rico VJ, Crespo A, et al. 2015. Molecular sequence data from populations of *Bryoria fuscescens* s.l. in the mountains of central Spain indicates a mismatch between haplotypes and chemotypes. *The Lichenologist* 47: 279–286.
- Boluda CG, Rico VJ, Hawksworth DL. 2014. Fluorescence microscopy as a tool for the visualization of lichen substances within *Bryoria thalii*. *The Lichenologist* 46: 723–726.
- Boni MF, Posada D, Feldman MW. 2007. An exact nonparametric method for inferring mosaic structure in sequence triplets. *Genetics* 176: 1035–1047.
- Brodo IM, Hawksworth DL. 1977. *Alectoria* and allied genera in North America. *Opera Botanica* 42: 1–164.
- Campbell V, Legendre P, Lapointe FJ. 2011. The performance of the congruence among distance matrices (CADM) test in phylogenetic analysis. *BMC Evolutionary Biology* 11: 64.
- Caparrós R, Lara F, Draper I, et al. 2016. Integrative taxonomy sheds light on an old problem: the *Ulota crispa* complex (Orthotrichaceae, Musci). *Botanical Journal of the Linnean Society* 180: 427–451.
- Chatrou LW, Escribano MP, Viruel MA, et al. 2009. Flanking regions of monomorphic microsatellite loci provide a new source of data for plant species-level phylogenetics. *Molecular Phylogenetics and Evolution* 53: 726–733.
- Clement M, Posada D, Crandall KA. 2000. TCS: a computer program to estimate gene genealogies. *Molecular Ecology* 9: 1657–1659.
- Crespo A, Lumbsch HT. 2010. Cryptic species in lichen-forming fungi. *IMA Fungus* 1: 167–170.
- Dal Grande F, Alors D, Pradeep KD, et al. 2014. Insights into intrathalline genetic diversity of the cosmopolitan lichen symbiotic green alga *Trebouxia decolorans* Ahmadjian using microsatellite markers. *Molecular Phylogenetics and Evolution* 72: 54–60.
- Darriba D, Taboada GL, Doallo R, et al. 2012. jModelTest 2: more models, new heuristics and parallel computing. *Nature Methods* 9: 772.
- Dayrat B. 2005. Towards integrative taxonomy. *Biological Journal of the Linnean Society* 85: 407–415.
- Del-Prado R, Divakar PK, Lumbsch HT, et al. 2016. Hidden genetic diversity in an asexually reproducing lichen forming fungal group. *PLoS ONE* 11: e0161031.
- Divakar PK, Cubas P, Blanco O, et al. 2010. An overview on hidden diversity in lichens: Parmeliaceae. http://taxateca.com/files/Divakar_et_al_2010.pdf.
- Divakar PK, Leavitt SD, Molina MC, et al. 2016. A DNA barcoding approach for identification of hidden diversity in Parmeliaceae (Ascomycota): *Parmelia sensu stricto* as a case study. *Botanical Journal of the Linnean Society* 180: 21–29.
- Douhan GW, Martin DP, Rizzo DM. 2007. Using the putative asexual fungus *Cenococcum geophilum* as a model to test how species concepts influence recombination analyses using sequence data from multiple loci. *Current Genetics* 52: 191–201.
- Drummond AJ, Rambaut A, Shapiro B, et al. 2005. Bayesian coalescent inference of past population dynamics from molecular sequences. *Molecular Biology and Evolution* 22: 1185–1192.
- Drummond AJ, Suchard MA, Xie D, et al. 2012. Bayesian phylogenetics with BEAUti and the BEAST 1.7. *Molecular Biology and Evolution* 29: 1969–1973.
- Earl DA, Von Holdt B. 2012. STRUCTURE HARVESTER: a website and program for visualizing STRUCTURE output and implementing the Evanno method. *Conservation of Genetics Resources* 4: 359–361.
- Edwards CE, Soltis DE, Soltis PS. 2008. Using patterns of genetic structure based on microsatellite loci to test hypotheses of current hybridization, ancient hybridization and incomplete lineage sorting in *Conradina* (Lamiaceae). *Molecular Ecology* 17: 5157–5174.
- Emelianov I, Marec F, Mallet J. 2004. Genomic evidence for divergence with gene flow in host races of the larch budmoth. *Proceedings of the Royal Society of London, Biological Sciences* 271: 97–105.
- Esseen PA, Olsson T, Coxson D, et al. 2015. Morphology influences water storage in hair lichens from boreal forest canopies. *Fungal Ecology* 18: 26–35.
- Esseen PA, Rönqvist M, Gauslaa Y, et al. 2017. Externally held water – a key factor for hair lichens in boreal forest canopies. *Fungal Ecology* 30: 29–38.
- Evanno G, Regnaut S, Goudet J. 2005. Detecting the number of clusters of individuals using the software STRUCTURE: a simulation study. *Molecular Ecology* 14: 2611–2620.
- Falush D, Stephens M, Pritchard J. 2003. Inference of population structure using multilocus genotype data: Linked loci and correlated allele frequencies. *Genetics* 155: 945–959.
- Färber L, Solhaug KA, Esseen PA, et al. 2014. Sunscreening fungal pigments influence the vertical gradient of pendulous lichens in boreal forest canopies. *Ecology* 95: 1464–1471.
- Fu YX. 1997. Statistical test of neutrality of mutations against population growth, hitchhiking and background selection. *Genetics* 147: 915–925.
- Gardes M, Bruns TD. 1993. ITS primers with enhanced specificity for basidiomycetes-application to the identification of mycorrhizae and rusts. *Molecular Ecology* 2: 113–118.
- Gargas A, Taylor JW. 1992. Polymerase chain reaction (PCR) primers for amplifying and sequencing nuclear 18S rDNA from lichenized fungi. *Mycologia* 84: 589–592.
- Gibbs MJ, Armstrong JS, Gibbs AJ. 2000. Sister-scanning: a Monte Carlo procedure for assessing signals in recombinant sequences. *Bioinformatics* 16: 573–582.
- Grant WS. 2015. Problems and cautions with sequence mismatch analysis and Bayesian skyline plots to infer historical demography. *Journal of Heredity* 16: 1–14.
- Hart WM, Sunday J. 2007. Things fall apart: biological species form unconnected parsimony networks. *Biology Letters* 3: 509–512.
- Hartl DL, Clark AG. 2007. *Principles of population genetics*. 4th Ed. Sinauer Associates Inc, Sunderland, MA.
- Hawksworth DL. 1969a. Chemical and nomenclatural notes on *Alectoria* (Lichenes) I. *Taxon* 18: 393–399.
- Hawksworth DL. 1969b. The scanning electron microscope, an aid to the study of cortical hyphal orientation in the lichen genera *Alectoria* and *Cornicularia*. *Journal de Microscopie* 8: 753–760.
- Hawksworth DL. 1972. Regional studies in *Alectoria* (Lichenes) II. The British species. *The Lichenologist* 5: 181–261.

- Hawksworth DL. 1976. Lichen chemotaxonomy. In: Brown DH, Hawksworth DL, Bailey LH (eds), *Lichenology: progress and problems*: 139–184. Academic Press, London.
- Hawksworth DL. 2015. Lichenization: The origins of fungal life-style. In: Upreti DK, Divakar PK, Shukla V, et al (eds), *Recent advances in lichenology. Modern methods and approaches in lichen systematics and culture techniques*, vol. 2: 1–10. Springer, India.
- Hawksworth DL, Jørgensen PM. 2013. (2196) Proposal to conserve the name *Alectoria fuscescens* (*Bryoria fuscescens*) against *Lichen chalybeiformis* and *Alectoria subcana* (Ascomycota: Lecanorales: Parmeliaceae). *Taxon* 62: 1057.
- Hawksworth DL, Lücking R. 2017. Fungal diversity revisited: 2.2 to 3.8 million species. *Microbiology Spectrum* 5: FUNK-0052-2016.
- Hey J. 2006. Recent advances in assessing gene flow between diverging populations and species. *Current Opinion in Genetics & Development* 16: 592–596.
- Hibbett DS. 2016. The invisible dimension of fungal diversity. *Science* 351: 1150–1151.
- Hobolth A, Duthel JY, Hawks J, et al. 2011. Incomplete lineage sorting patterns among human, chimpanzee, and orangutan suggest recent orangutan speciation and widespread selection. *Genome Research* 21: 349–356.
- Holderegger R, Kamm U, Gugerli F. 2006. Adaptive vs neutral genetic diversity: implications for landscape genetics. *Landscape Ecology* 21: 797–807.
- Houbraken J, Frisvad JC, Seifert KA, et al. 2012. New penicillin-producing *Penicillium* species and an overview of section *Chrysogena*. *Persoonia* 29: 78–100.
- Huelsenbeck JP, Ronquist F. 2001. MrBayes: Bayesian inference of phylogenetic trees. *Bioinformatics* 17: 754–755.
- Jakob SS, Blattner FR. 2006. A chloroplast genealogy of *Hordeum* (Poaceae): Long-term persisting haplotypes, incomplete lineage sorting, regional extinction, and the consequences for phylogenetic inference. *Molecular Biology and Evolution* 23: 1602–1612.
- Jakobsson M, Rosenberg NA. 2007. CLUMMP: a cluster matching and permutation program for dealing with label switching and multimodality in analysis of population structure. *Bioinformatics* 23: 1801–1806.
- Joly S, McLenachan PA, Lockhart PJ. 2009. A statistical approach for distinguishing hybridization and incomplete lineage sorting. *The American Naturalist* 174: E54–E70.
- Jones G, Aydin Z, Oxelman B. 2014. DISSECT: an assignment-free Bayesian discovery method for species delimitation under the multispecies coalescent. *Bioinformatics* 31: 991–998.
- Jørgensen PM, Galloway DJ. 1983. *Bryoria* (lichenized Ascomycota) in New Zealand. *New Zealand Journal of Botany* 21: 335–340.
- Kaasalainen U, Heinrichs J, Krings M, et al. 2015. Alectoroid morphologies in Paleogene lichens: new evidence and re-evaluation of the fossil *Alectoria succini* Mägdefrau. *PLoS ONE* 10: e0129526.
- Katoh K, Standley DM. 2013. MAFFT multiple sequence alignment software version 7: improvements in performance and usability. *Molecular Biology and Evolution* 30: 772–780.
- Kay KM, Whittall JB, Scott AH. 2006. A survey of nuclear ribosomal internal transcribed spacer substitution rates across angiosperms: an approximate molecular clock with life history effects. *BMC Evolutionary Biology* 6: 36.
- Keller C, Scheidegger C. 2016. Multiple mating events and spermatia-mediated gene flow in the lichen-forming fungus *Lobaria pulmonaria*. *Herzogia* 29: 435–450.
- Keller NP, Hohn TM. 1997. Metabolic pathway gene clusters in filamentous fungi. *Fungal Genetics and Biology* 21: 17–21.
- Kirika P, Divakar PK, Crespo A, et al. 2016a. Polyphyly of the genus *Canothecium* – uncovering incongruences between phenotype-based classification and molecular phylogeny within lichenized Ascomycota (Parmeliaceae). *Phytotaxa* 289: 36–48.
- Kirika P, Divakar PK, Crespo A, et al. 2016b. Phylogenetic studies uncover a predominantly African lineage in a widely distributed lichen-forming fungal species. *Mycologia* 14: 1–16.
- Knowles LL. 2008. Why does a method that fails continue to be used. *Evolution* 62: 2713–2717.
- Konrad H, Kiristis T, Riegler M, et al. 2002. Genetic evidence for natural hybridization between the Dutch elm disease pathogens *Ophiostoma novo-ulmi* ssp. *novo-ulmi* and *O. novo-ulmi* ssp. *americana*. *Plant Pathology* 51: 78–84.
- Kroken S, Taylor JW. 2001a. Outcrossing and recombination in the lichenized fungus *Letharia*. *Fungal Genetics and Biology* 34: 83–92.
- Kroken S, Taylor JW. 2001b. A gene genealogical approach to recognize phylogenetic species boundaries in the lichenized fungus *Letharia*. *Mycologia* 93: 38–53.
- Lamichaney S, Berglund J, Markus SA, et al. 2015. Evolution of Darwin's finches and their beaks revealed by genome sequencing. *Nature* 518: 371–375.
- Lanfear R, Calcott B, Ho SY, et al. 2012. Partitionfinder: combined selection of partitioning schemes and substitution models for phylogenetic analyses. *Molecular Biology and Evolution* 29: 1695–1701.
- Leavitt SD, Divakar PK, Crespo A, et al. 2016. A matter of time – understanding the limits of the power of molecular data for delimiting species boundaries. *Herzogia* 29: 479–492.
- Leavitt SD, Esslinger TL, Divakar PK, et al. 2012a. Miocene and Pliocene dominated diversification of the lichen-forming fungal genus *Melanohalea* (Parmeliaceae, Ascomycota) and Pleistocene population expansions. *BMC Evolutionary Biology* 12: 176.
- Leavitt SD, Esslinger TL, Lumbsch HT. 2012b. Neogene-dominated diversification in neotropical montane lichens: Dating divergence events in the lichen-forming fungal genus *Oropogon* (Parmeliaceae). *American Journal of Botany* 99: 1764–1777.
- Leavitt SD, Grewe F, Widhelm T, et al. 2016. Resolving evolutionary relationships in lichen-forming fungi using diverse phylogenomic datasets and analytical approaches. *Scientific Reports* 6: 22262.
- Leavitt SD, Johnson L, St. Clair LL. 2011. Species delimitation and evolution in morphologically and chemically diverse communities of the lichen-forming genus *Xanthoparmelia* (Parmeliaceae, Ascomycota) in Western North America. *American Journal of Botany* 98: 175–188.
- Legendre P, Lapointe FJ. 2004. Assessing congruence among distance matrices: Single-malt Scotch whiskeys revisited. *Australian & New Zealand Journal of Statistics* 46: 615–629.
- Librado P, Rozas J. 2009. DnaSP v5: A software for comprehensive analysis of DNA polymorphism data. *Bioinformatics* 25: 1451–1452.
- Lindgren H, Velmala S, Högnabba F, et al. 2014. High fungal selectivity for algal symbionts in the genus *Bryoria*. *The Lichenologist* 46: 681–695.
- Lumbsch HT. 1988. The use of metabolic data in lichenology at the species and subspecific levels. *The Lichenologist* 30: 357–367.
- Lumley LM, Sperling FAH. 2011. Utility of microsatellites and mitochondrial DNA for species delimitation in the spruce budworm (*Choristoneura fumiferana*) species complex (Lepidoptera: Tortricidae). *Molecular Phylogenetics and Evolution* 58: 232–243.
- Lutsak T, Fernández-Mendoza F, Nadyeina O, et al. 2017. Testing the correlation between norstictic acid content and species evolution in the *Cetraria aculeata* group in Europe. *The Lichenologist* 49: 39–56.
- Maddison WP. 1997. Gene trees in species trees. *Systematic Biology* 46: 523–536.
- Maechler M, Rousseeuw P, Struyf A, et al. 2013. *cluster: Cluster Analysis Basics and Extensions*. R package version 1.14.4.
- Majerus MEN. 2009. Industrial melanism in the Peppered Moth, *Biston betularia*: An excellent teaching example of Darwinian evolution in action. *Evolution: Education and Outreach* 2: 63–74.
- Mark K, Saag L, Leavitt SD, et al. 2016. Evaluation of traditionally circumscribed species in the lichen-forming genus *Usnea*, section *Usnea* (Parmeliaceae, Ascomycota) using six-locus dataset. *Organisms Diversity and Evolution* 16: 497–524.
- Martin DP, Lemey P, Lott M, et al. 2010. RDP3: a flexible and fast computer program for analyzing recombination. *Bioinformatics* 26: 2462–2463.
- Martin DP, Posada D, Crandall KA, et al. 2005. A modified bootscan algorithm for automated identification of recombinant sequences and recombination breakpoints. *AIDS Research and Human Retroviruses* 21: 98–102.
- Martin DP, Rybicki E. 2000. RDP: detection of recombination amongst aligned sequences. *Bioinformatics* 16: 562–563.
- Maynard-Smith J. 1992. Analyzing the mosaic structure of genes. *Journal of Molecular Evolution* 34: 126–129.
- McGuire JA, Linkem CW, Koo MS, et al. 2007. Mitochondrial introgression and incomplete lineage sorting through space and time: Phylogenetics of crotaphytid lizards. *Evolution* 61: 2879–2897.
- McMullin RT, Lendemer JC, Braid HE, et al. 2016. Molecular insights into the lichen genus *Alectoria* (Parmeliaceae) in North America. *Botany* 94: 1–11.
- Miller MA, Pfeiffer W, Schwartz T. 2010. Creating the CIPRES Science Gateway for inference of large phylogenetic trees. In: *Proceedings of the Gateway Computing Environments Workshop (GCE)*, November 14: 1–8. USA, New Orleans.
- Modica MV, Puillandre N, Castelin M, et al. 2014. A good compromise: rapid and robust species proxies for inventorying biodiversity hotspots using the Terebridae (Gastropoda: Conoidea). *PLoS ONE*: e012160.
- Molina MC, Del-Prado R, Divakar PK, et al. 2011a. Another example of cryptic diversity in lichen-forming fungi: the new species *Parmelia mayi* (Ascomycota: Parmeliaceae). *The Lichenologist* 11: 331–342.
- Molina MC, Divakar PK, Goward T, et al. 2016. Neogene diversification in the temperate lichen-forming fungal genus *Parmelia* (Parmeliaceae, Ascomycota). *Systematics and Biodiversity* 15: 166–181.
- Molina MC, Divakar PK, Millanes AM, et al. 2011b. *Parmelia sulcata* (Ascomycota: Parmeliaceae), a sympatric monophyletic species complex. *The Lichenologist* 43: 585–601.

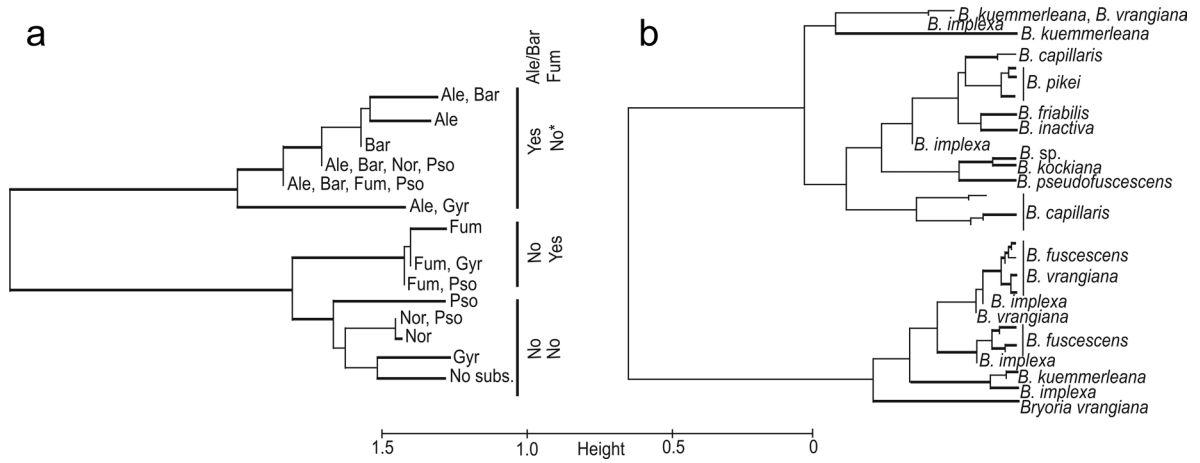
- Monaghan MT, Wild R, Elliot M, et al. 2009. Accelerated species inventory on Madagascar using coalescent-based models of species delineation. *Systematic Biology* 58: 298–311.
- Motyka J. 1964. The North American species of *Alectoria*. *The Bryologist* 67: 1–44.
- Myllys L, Lindgren H, Aikio S, et al. 2016. Chemical diversity and ecology of the genus *Bryoria* section *Implexae* (Parmeliaceae) in Finland. *The Bryologist* 119: 29–38.
- Myllys L, Stenroos S, Thell A. 2002. New genes for phylogenetic studies of lichenized fungi: glyceraldehyde-3-phosphate dehydrogenase and beta-tubulin genes. *The Lichenologist* 34: 237–246.
- Myllys L, Velmala S, Holien H, et al. 2011. Phylogeny of the genus *Bryoria*. *The Lichenologist* 6: 617–638.
- Naciri Y, Linder HP. 2015. Species delimitation and relationships: The dance of seven veils. *Taxon* 64: 3–16.
- Nadyeina O, Cornejo C, Boluda CG, et al. 2014. Characterization of micro-satellite loci in lichen-forming fungi of *Bryoria* section *Implexae* (Parmeliaceae). *Applied Plant Sciences* 2: 1400037.
- Nichols R. 2001. Gene trees and species trees are not the same. *Trends in Ecology & Evolution* 16: 358–364.
- Oberwinkler F. 2017. Yeasts in Pucciniomycotina. *Mycological Progress* 16: 831–856.
- Orange A, James PW, White FJ. 2010. Microchemical methods for the identification of lichens. 2 edn. British Lichen Society, London.
- Padidam M, Sawyer S, Fauquet CM. 1999. Possible emergence of new geminiviruses by frequent recombination. *Virology* 265: 218–225.
- Paradis E, Claude J, Strimmer K. 2004. APE: analyses of phylogenetics and evolution in R language. *Bioinformatics* 20: 289–290.
- Parnmen S, Leavitt SD, Rangsiruji A, et al. 2013. Identification of species in the *Cladia aggregata* group using DNA barcoding (Ascomycota: Lecanorales). *Phytotaxa* 115: 1–14.
- Pažoutová S, Pešicová K, Chudíčková M, et al. 2015. Delimitation of cryptic species inside *Claviceps purpurea*. *Fungal Biology* 119: 7–26.
- Perelman P, Johnson WE, Roos C, et al. 2011. A molecular phylogeny of living primates. *PLoS Genetics* 7: e1001342.
- Pino-Bodas R, Pérez-Vargas I, Stenroos S, et al. 2016. Sharpening the species boundaries in the *Cladonia mediterranea* complex (Cladoniaceae, Ascomycota). *Persoonia* 37: 1–12.
- Pons J, Barraclough TG, Gómez-Zurita J, et al. 2006. Sequence based species delimitation for the DNA taxonomy of undescribed insects. *Systematic Biology* 55: 595–609.
- Posada D, Crandall KA. 2001. Evaluation of methods for detecting recombination from DNA sequences: computer simulations. *Proceedings of the National Academy of Sciences of the United States of America* 98: 13757–13762.
- Printzen C, Ekman S. 2002. Genetic variability and its geographical distribution in the widely disjunct *Cavernularia hultenii*. *The Lichenologist* 34: 101–111.
- Pritchard JK, Stephens M, Donnelly P. 2000. Inference of population structure using multilocus genotype data. *Genetics* 155: 945–959.
- Puillandre N, Lambert A, Brouillet S, et al. 2011. ABGD, Automatic Barcode Gap Discovery for primary species delimitation. *Molecular Ecology* 21: 1864–1877.
- R Core Team. 2014. R: A language and environment for statistical computing. Vienna, R Foundation for Statistical Computing.
- Rambaut A. 2009. FigTree v.1.4. <http://tree.bio.ed.ac.uk/software/figtree/>.
- Rambaut A, Suchard MA, Xie D, et al. 2014. Tracer. Version 1.6. <http://beast.bio.ed.ac.uk/Tracer>.
- Ronquist F, Huelsenbeck JP. 2003. MrBayes 3: Bayesian phylogenetic inference under mixed models. *Bioinformatics* 19: 1572–1574.
- Rosenberg NA. 2003. The shapes of neutral gene genealogies in two species: Probabilities of monophyly, paraphyly, and polyphyly in a coalescence model. *Evolution* 57: 1465–1477.
- Saag L, Mark K, Saag A, et al. 2014. Species delimitation in the lichenized fungal genus *Vulpicida* (Parmeliaceae, Ascomycota) using gene concatenation and coalescent-based species tree approaches. *American Journal of Botany* 101: 2169–2182.
- Schoch CL, Seifert KA, Huhndorf S, et al. 2012. Nuclear ribosomal internal transcribed spacer (ITS) region as a universal DNA barcode for fungi. *Proceedings of the National Academy of Sciences of the United States of America* 109: 6241–6246.
- Schoustra SE, Debets AJM, Slakhorst M, et al. 2007. Mitotic recombination accelerates adaptation in the fungus *Aspergillus nidulans*. *PLoS Genetics* 3: e68 APR.
- Seymour FA, Crittenden PD, Wirtz N, et al. 2007. Phylogenetic and morphological analysis of Antarctic lichen-forming *Usnea* species in the group *Neurospogon*. *Antarctic Science* 19: 71–82.
- Singh G, Dal Grande F, Cornejo C, et al. 2012. Genetic basis of self-incompatibility in the lichen-forming fungus *Lobaria pulmonaria* and skewed frequency distribution of mating-type idiomorphs: Implications for conservation. *PloS ONE* 7: e51402.
- Singh G, Dal Grande F, Divakar PK, et al. 2015. Coalescent-based species delimitation approach uncovers high cryptic diversity in the cosmopolitan lichen-forming fungal genus *Protopermella* (Lecanorales, Ascomycota). *PLoS ONE* 10: e0124625.
- Spribile T, Touvinen V, Resl P, et al. 2016. Basidiomycete yeasts in the cortex of ascomycete macrolichens. *Science*. doi: <https://doi.org/10.1126/science.aaf8287>.
- Stamatakis A. 2006. RaxML-VI-HPC: maximum likelihood-based phylogenetic analyses with thousands of taxa and mixed models. *Bioinformatics* 22: 2688–2690.
- Stamatakis A. 2014. RaxML version 8: A tool for phylogenetic analysis and post-analysis of large phylogenies. *Bioinformatics* 30: 1312–1313.
- Stamatakis A, Hoover P, Rougemont J. 2008. A rapid bootstrap algorithm for the RAXML web servers. *Systematic Biology* 57: 758–771.
- Steinová J, Stenroos S, Grube M, et al. 2013. Genetic diversity and species delimitation of the zeorin-containing red-fruited *Cladonia* species (lichenized Ascomycota) assessed with ITS rDNA and β -tubulin data. *The Lichenologist* 45: 665–684.
- Stewart JE, Timmer LW, Lawrence CB, et al. 2014. Discord between morphological and phylogenetic species boundaries: incomplete lineage sorting and recombination results in fuzzy species boundaries in an asexual fungal pathogen. *BMC Evolutionary Biology* 14: 38.
- Stuessy TF. 2009. Plant taxonomy. The systematic evaluation of comparative data. Columbia University Press, New York.
- Suzuki R, Shimodaira H. 2006. pvcust: an R package for assessing the uncertainty in hierarchical clustering. *Bioinformatics* 22: 1540–1542.
- Tajima F. 1989. Statistical method for testing the neutral mutation hypothesis by DNA polymorphism. *Genetics* 123: 585–595.
- Tamura K, Peterson D, Peterson N, et al. 2011. MEGA5: Molecular evolutionary genetics analysis using maximum likelihood, evolutionary distance, and maximum parsimony methods. *Molecular Biology and Evolution* 28: 2731–2739.
- Templeton AR. 2009. Why does a method that fails continue to be used: the answer. *Evolution* 63: 807–812.
- Thomas NT, Krings M, Taylor EL. 2014. Fossil fungi. Academic Press, London.
- Turland NJ, Wiersma JH, Barrie FR, et al. (eds). 2018. International Code of Nomenclature for algae, fungi, and plants (Shenzhen Code) adopted by the Nineteenth International Botanical Congress Shenzhen, China, July 2017. [Regnum Vegetabile no. 159.] Königstein, Koeltz Botanical Books.
- Vanhaeche D, García de Leaniz C, Gajardo G, et al. 2012. DNA barcoding and microsatellites help species delimitation and hybrid identification in endangered galaxiid fishes. *PLoS ONE* 7: e32939.
- Velmala S, Myllys L, Goward T, et al. 2014. Taxonomy of *Bryoria* section *Implexae* (Parmeliaceae, Lecanoromycetes) in North America and Europe, based on chemical, morphological and molecular data. *Annales Botanici Fennici* 51: 345–371.
- Weiller GF. 1998. Phylogenetic profiles: a graphical method for detecting genetic recombination in homologous sequences. *Molecular Biology and Evolution* 15: 326–335.
- White TJ, Bruns T, Lee S, et al. 1990. Amplification and direct sequencing of fungal ribosomal RNA genes for phylogenetics. In: Innis MA, Gelfand DH, Sninsky JJ, et al. (eds), PCR protocols: a guide to methods and applications: 315–322. New York: Academic Press.
- Widmer I, Dal Grande F, Excoffier L, et al. 2012. European phylogeography of the epiphytic lichen fungus *Lobaria pulmonaria* and its green algal symbiont. *Molecular Ecology* 21: 5827–5844.
- Will KW, Mishler BD, Wheeler QD. 2005. The perils of DNA barcoding and the need for integrative taxonomy. *Systematic Biology* 54: 844–851.
- Zamora JC, Calonge FD, Martín MP. 2013. New sources of taxonomic information for earthstars (Geastrum, Geastraceae, Basidiomycota): phenoloxidases and rhizomorph crystals. *Phytotaxa* 132: 1–20.
- Zamora JC, Calonge FD, Martín MP. 2015. Integrative taxonomy reveals an unexpected diversity in *Geastrum* section *Geastrum* (Geastrales, Basidiomycota). *Persoonia* 34: 130–165.
- Zardoya R, Vollmer DM, Craddock C, et al. 1996. Evolutionary conservation of microsatellite flanking regions and their use in resolving the phylogeny of cichlid fishes (Pisces: Perciformes). *Proceedings of the Royal Society, Biological Sciences* 263: 1589–1598.
- Zhang J, Kapli P, Pavlidis P, et al. 2013. A general species delimitation method with applications to phylogenetic placements. *Bioinformatics* 29: 2869–2876.
- Zoller S, Lutzoni F, Scheidegger C. 1999. Genetic variation within and among populations of the threatened lichen *Lobaria pulmonaria* in Switzerland and implications for its conservation. *Molecular Ecology* 8: 2049–2059.

Appendix 1 Chemical, geographical and morphological characters used of *Bryoria* sect. *Implexae* samples in the phenogram reconstruction (Fig. 1).

Samples	Alectorialic acid	Barbatolic acid	Fumarprotocetraric acid	Gyrophoric acid	Norsitctic acid	Psoromic acid	Old World (0) / New World (1)	Thallus brownish (0) / whitish (1)	Branching angles acute	Branching angles obtuse	Soralia fissural	Soralia tuberculate	Pseudocyphellae inconspicuous (0) / conspicuous (1)
capillaris_L01-17	1	1	0	0	0	0	0	0	1	0	0	0	0
capillaris_L06-10	1	1	0	0	0	0	0	0	1	0	0	0	1
capillaris_L07-15	1	1	0	0	0	0	0	0	1	1	0	0	0
capillaris_L08-12	1	1	0	0	0	0	0	0	1	0	0	1	0
capillaris_L13-03	1	1	0	0	0	0	0	0	1	1	0	1	0
capillaris_L14-02	1	1	1	0	0	1	0	0	1	1	0	0	1
capillaris_L141	1	1	0	0	0	0	0	0	1	0	0	1	0
capillaris_L15-15	1	1	0	0	0	0	0	0	1	0	0	0	0
capillaris_L16-21	1	1	0	0	1	1	0	0	1	1	0	0	0
capillaris_L211	1	1	0	0	0	0	0	0	1	0	0	1	0
capillaris_L270	0	1	0	0	0	0	0	0	1	0	0	1	0
capillaris_S192	1	1	0	0	0	0	0	0	1	0	0	1	0
capillaris_S2	1	1	0	0	0	0	0	0	1	0	0	1	0
friabilis_02	0	0	0	1	0	0	1	1	1	0	0	0	1
friabilis_L355	0	0	0	1	0	0	1	1	1	0	0	0	1
friabilis_L407	0	0	0	1	0	0	1	1	1	0	0	0	1
friabilis_S395	0	0	0	1	0	0	1	1	1	0	0	0	1
fuscescens_L12-03	0	0	1	0	0	0	0	1	1	0	1	1	0
fuscescens_L12-05	0	0	1	0	0	0	0	1	0	1	1	1	0
fuscescens_L139	0	0	1	0	0	0	0	1	1	0	1	1	0
fuscescens_L149	0	0	1	0	0	0	0	1	1	0	1	1	0
fuscescens_L15-21	0	0	1	0	0	0	0	1	1	1	1	1	0
fuscescens_L160	0	0	1	0	0	0	0	1	1	0	1	1	0
fuscescens_L189	0	0	1	0	0	0	0	1	1	0	1	1	0
fuscescens_L224	0	0	1	0	0	0	0	1	1	0	1	1	0
fuscescens_L232	0	0	0	0	0	0	0	1	1	0	1	1	0
fuscescens_L305	0	0	1	0	0	0	0	1	1	0	1	1	0
fuscescens_S109	0	0	1	0	0	0	0	1	1	0	1	1	0
fuscescens_S157	0	0	1	0	0	0	0	1	1	0	1	1	0
fuscescens_S24	0	0	1	0	0	0	0	1	1	0	1	1	0
fuscescens_S256	0	0	1	0	0	0	1	1	1	0	1	1	0
fuscescens_S259	0	0	1	0	0	0	1	1	1	0	1	1	0
fuscescens_S260a	0	0	1	0	0	0	1	1	1	0	1	1	0
fuscescens_S261	0	0	1	0	0	0	1	1	1	0	1	1	0
fuscescens_S267	0	0	1	0	0	0	1	1	1	0	1	1	0
fuscescens_S272	0	0	1	0	0	0	1	1	1	0	1	1	0
fuscescens_S274	0	0	0	0	0	0	1	1	1	0	1	1	0
fuscescens_S369	0	0	1	0	0	0	1	1	1	0	1	1	0
fuscescens_S379	0	0	1	0	0	0	1	1	1	0	1	1	0
fuscescens_S380	0	0	1	0	0	0	1	1	1	0	1	1	0
fuscescens_S56	0	0	1	0	0	0	0	1	1	0	1	1	0
implexa_L01-01	0	0	0	0	0	1	0	1	1	1	1	1	1
implexa_L06-05	0	0	1	0	0	1	0	1	1	0	0	1	0
implexa_L10-03	0	0	0	0	0	1	0	1	0	1	0	0	1
implexa_L11-15	0	0	0	0	0	1	0	1	0	1	0	1	0
implexa_L16-15	0	0	0	0	0	1	0	1	1	0	0	0	1
implexa_S168	0	0	0	0	0	1	0	1	1	1	1	1	1
implexa_S22	0	0	0	0	0	1	0	1	1	1	1	1	1
implexa_S36	0	0	0	0	0	1	0	1	1	1	1	1	1
implexa_S39	0	0	0	0	0	1	0	1	1	1	1	1	1
implexa_S67	0	0	0	0	0	1	0	1	1	1	1	1	1
inactiva_L206	0	0	0	0	0	0	1	0	1	0	0	0	1
inactiva_L323b	0	0	0	0	0	0	1	0	1	0	0	0	1
inactiva_L347	0	0	0	0	0	0	1	0	1	0	0	0	1
inactiva_L358	0	0	0	0	0	0	1	0	1	0	0	0	1
inactiva_S239a	0	0	0	0	0	0	1	0	1	0	0	0	1
inactiva_S384	0	0	0	0	0	0	1	0	1	0	0	0	1
inactiva_S392	0	0	0	0	0	0	1	0	1	0	0	0	1
kockiana_L394	0	0	0	0	0	1	1	0	1	1	0	0	0
kockiana_L396	0	0	0	0	0	1	1	0	1	1	0	0	0
kuemmerleana_L04-03	0	0	0	0	1	0	0	1	1	0	0	0	0
kuemmerleana_L09-04	0	0	0	0	1	0	0	1	1	1	0	0	1
kuemmerleana_L09-07	0	0	0	0	1	0	0	1	1	0	0	0	0
kuemmerleana_L16-17	0	0	0	0	1	1	0	1	1	1	1	1	1
kuemmerleana_L244	0	0	0	0	1	0	0	1	1	1	1	1	1
kuemmerleana_L274	0	0	0	0	1	0	0	1	1	1	1	1	1
kuemmerleana_L275	0	0	0	0	1	0	0	1	1	1	1	1	1

Appendix 1 (cont.)

Samples	Alectorialic acid	Barbatolic acid	Fumarprotocetraric acid	Gyrophoric acid	Norstictic acid	Psoromic acid	Old World (0) / New World (1)	Thallus brownish (0) / whitish (1)	Branching angles acute	Branching angles obtuse	Soralia fissural	Soralia tuberculate	Pseudocyphellae inconspicuous (0) / conspicuous (1)
kuemmerleana_S128	0	0	0	0	1	0	0	1	1	1	1	1	1
kuemmerleana_S160	0	0	0	0	1	0	0	1	1	1	1	1	1
pikei_02	1	1	0	0	0	0	1	1	1	0	0	0	1
pikei_04	1	1	0	0	0	0	1	1	1	0	0	0	1
pikei_05	1	1	0	0	0	0	1	1	1	0	0	0	1
pikei_07	1	1	0	0	0	0	1	1	1	0	0	0	1
pikei_09	1	1	0	0	0	0	1	1	1	0	0	0	1
pikei_10	1	1	0	0	0	0	1	1	1	0	0	0	1
pikei_11	1	1	0	0	0	0	1	1	1	0	0	0	1
pikei_12	1	1	0	0	0	0	1	1	1	0	0	0	1
pikei_13	1	1	0	0	0	0	1	1	1	0	0	0	1
pikei_14	1	1	0	0	0	0	1	1	1	0	0	0	1
pikei_15	1	1	0	0	0	0	1	1	1	0	0	0	1
pikei_a	1	1	0	0	0	0	1	1	1	0	0	0	1
pikei_b	1	1	0	0	0	0	1	1	1	0	0	0	1
pikei_c	1	0	0	0	0	0	1	1	1	0	0	0	1
pikei_d	1	1	0	0	0	0	1	1	1	0	0	0	1
pikei_L197	1	1	0	0	0	0	1	1	1	0	0	0	1
pikei_L210	1	1	0	0	0	0	1	1	1	0	0	0	1
pikei_L241	1	0	0	0	0	0	1	1	1	0	0	0	1
pikei_L374	1	0	0	1	0	0	1	1	1	0	0	0	1
pikei_L376	1	0	0	1	0	0	1	1	1	0	0	0	1
pikei_L377	1	0	0	1	0	0	1	1	1	0	0	0	1
pikei_S221	1	1	0	0	0	0	1	1	1	0	0	0	1
pikei_S362	1	1	0	0	0	0	1	1	1	0	0	0	1
pikei_S368	1	1	0	0	0	0	1	1	1	0	0	0	1
pikei_S382	1	1	0	0	0	0	1	1	1	0	0	0	1
pikei_S383a	1	1	0	0	0	0	1	1	1	0	0	0	1
pikei_S390	1	1	0	0	0	0	1	1	1	0	0	0	1
pikei_S394	1	1	0	0	0	0	1	1	1	0	0	0	1
pseudofuscenscens_S222	0	0	0	0	1	0	1	0	1	1	0	0	1
pseudofuscenscens_S232	0	0	0	0	1	0	1	0	1	1	0	0	1
pseudofuscenscens_S370	0	0	0	0	1	0	1	0	1	1	0	0	1
pseudofuscenscens_S371	0	0	0	0	1	0	1	0	1	1	0	0	1
pseudofuscenscens_S377	0	0	0	0	1	0	1	0	1	1	0	0	1
pseudofuscenscens_S386	0	0	0	0	1	0	1	0	1	1	0	0	1
pseudofuscenscens_S387	0	0	0	0	1	0	1	0	1	1	0	0	1
sp_L395	0	0	0	0	0	0	1	0	1	1	0	0	0
sp_S392	0	0	0	0	0	0	1	0	1	1	0	0	0
vrangiana_L02-20	0	0	1	0	0	0	0	1	0	1	1	1	0
vrangiana_L03-07	0	0	1	0	0	0	0	1	0	1	0	1	0
vrangiana_L05-17	0	0	1	0	0	0	0	1	0	1	0	1	0
vrangiana_L07-03	0	0	1	0	0	0	0	1	1	1	1	1	1
vrangiana_L07-19	0	0	0	0	0	0	0	1	0	1	0	0	0
vrangiana_L08-19	0	0	0	0	0	0	0	1	0	1	1	1	0
vrangiana_L08-20	0	0	1	0	0	0	0	1	0	1	0	1	0
vrangiana_L10-13	0	0	0	0	0	0	0	1	0	1	0	0	0
vrangiana_L12-11	0	0	1	1	0	0	0	1	0	1	1	1	0
vrangiana_L13-12	0	0	0	1	0	0	0	1	1	1	0	0	1
vrangiana_L272	0	0	0	1	0	0	0	1	0	1	1	1	0
vrangiana_L273	0	0	0	0	0	0	0	1	0	1	1	1	0
vrangiana_L300	0	0	0	0	0	0	0	1	0	1	1	1	0
vrangiana_L307	0	0	0	1	0	0	0	1	0	1	1	1	0
vrangiana_S10	0	0	0	1	0	0	0	1	0	1	1	1	0
vrangiana_S164	0	0	0	0	0	0	0	1	0	1	1	1	0
vrangiana_S166	0	0	1	0	0	0	0	1	0	1	1	1	0
vrangiana_S196a	0	0	0	0	0	0	0	1	0	1	1	1	0
vrangiana_S341	0	0	0	0	0	0	0	1	0	1	1	1	0
vrangiana_S385	0	0	1	0	0	0	0	1	0	1	1	1	0
vrangiana_S42	0	0	0	1	0	0	0	1	0	1	1	1	0
vrangiana_S45	0	0	0	0	0	0	0	1	0	1	1	1	0
vrangiana_S57	0	0	1	0	0	0	0	1	0	1	1	1	0
vrangiana_S59	0	0	1	0	0	0	0	1	0	1	1	1	0
vrangiana_S6	0	0	1	0	0	0	0	1	0	1	1	1	0
vrangiana_S62	0	0	0	1	0	0	0	1	0	1	1	1	0
vrangiana_S72	0	0	0	0	0	0	0	1	0	1	1	1	0



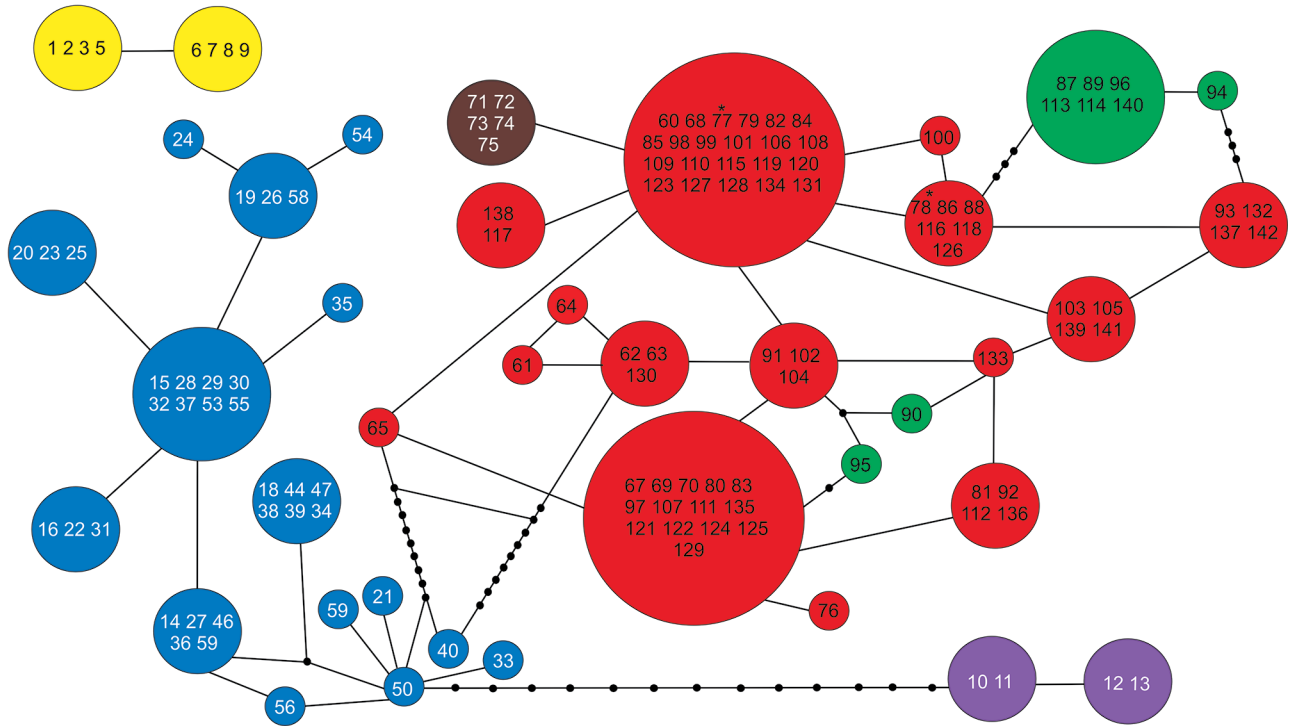
Appendix 2 Phenograms based on a presence/absence distance matrix in *Bryoria* sect. *Implexae* from: a. Extrolite composition alone; b. extrolite composition, with geographical, and morphological data. — **Bold** branches represent supported clades (bootstrap $\geq 70\%$, approximately unbiased $\geq 95\%$). — Ale. = Alecatorialic acid; Bar. = Barbatolic acid; Fum. = Fumarprotocetraric acid; Gyr. = Gyrophoric acid; No subs. = No substances detected; Nor. = Norstictic acid; Pso. = Psoromic acid; * = Except specimen named *Bryoria capillaris* L14.02.

Appendix 3 Microsatellite fragment lengths of *Bryoria* sect. *Implexae* analysed specimens.

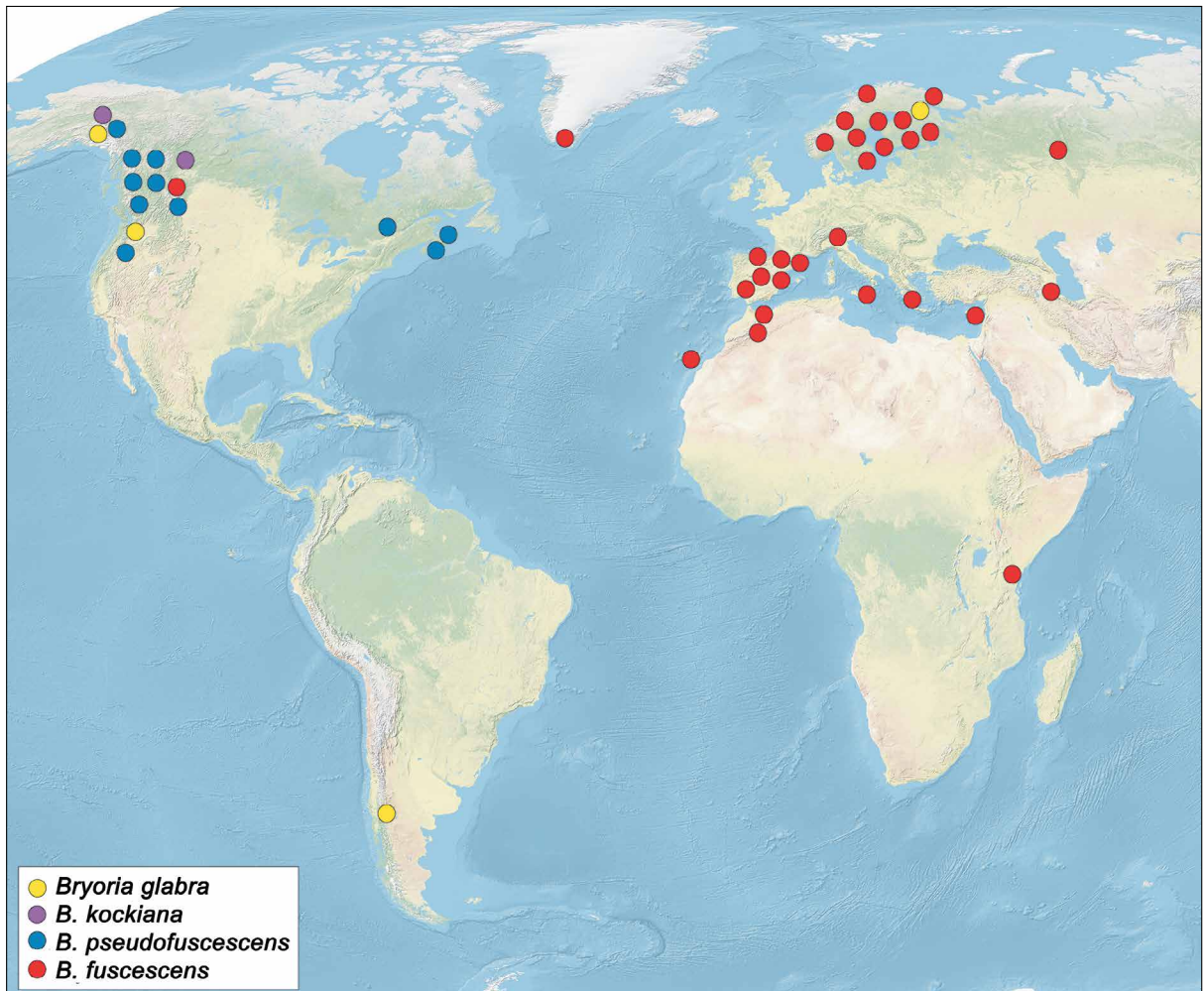
Sample	Bi01	Bi03	Bi04	Bi05	Bi10	Bi11	Bi12	Bi14	Bi19
capillaris_L01-17	103	279	323	128	437	316	100	365	346
capillaris_L06-10	103	279	323	128	437	316	100	365	346
capillaris_L07-15	103	279	323	128	437	316	100	365	346
capillaris_L08-12	103	279	323	128	434	316	103	361	346
capillaris_L13-03	94	279	325	138	434	318	115	361	346
capillaris_L14-02	112	279	327	128	437	320	100	365	346
capillaris_L141	123	281	323	136	434	316	100	361	346
capillaris_L15-15	112	279	323	–	437	316	100	365	346
capillaris_L16-21	103	279	323	128	437	316	100	365	346
capillaris_L211	112	279	323	136	434	316	103	361	346
capillaris_L270	112	279	323	138	434	316	124	361	346
capillaris_S192	112	279	323	128	437	316	100	365	346
capillaris_S2	94	279	323	138	434	316	124	361	346
friabilis_02	114	281	317	137	434	310	100	–	350
friabilis_L355	120	277	316	137	436	310	100	365	350
friabilis_L407	132	281	316	137	434	310	131	365	346
friabilis_S395	109	277	316	132	438	310	100	365	350
fuscescens_L12-03	112	279	323	138	434	316	103	361	352
fuscescens_L12-05	94	281	323	138	434	316	103	361	350
fuscescens_L139	94	279	323	138	434	316	103	361	352
fuscescens_L149	123	279	323	138	434	316	103	361	350
fuscescens_L15-21	123	277	325	138	434	318	115	361	352
fuscescens_L160	94	281	323	136	434	316	103	361	352
fuscescens_L189	112	279	323	138	434	316	100	361	352
fuscescens_L224	112	279	323	138	434	316	103	361	352
fuscescens_L232	94	279	323	138	434	316	103	361	352
fuscescens_L305	117	279	323	138	434	316	137	361	352
fuscescens_S109	112	281	323	138	434	316	118	361	350
fuscescens_S157	117	279	323	136	434	316	103	361	350
fuscescens_S24	112	281	323	138	434	316	106	361	352
fuscescens_S256	94	281	323	–	434	316	124	363	354
fuscescens_S259	94	277	323	138	437	316	103	363	352
fuscescens_S260a	82	279	323	138	437	316	103	363	352
fuscescens_S261	82	279	323	138	437	316	103	363	352
fuscescens_S267	82	279	323	138	437	316	103	363	352
fuscescens_S272	82	279	323	138	437	316	103	363	352
fuscescens_S274	94	279	323	138	434	316	–	361	350
fuscescens_S369	–	279	323	138	437	316	103	363	352
fuscescens_S379	94	279	323	138	437	316	100	363	352
fuscescens_S380	112	279	323	138	434	316	118	361	352
fuscescens_S56	123	279	323	136	434	316	100	361	350
glabra_01	114	283	306	132	426	299	115	369	344
glabra_02	120	283	306	132	426	299	–	369	344
glabra_03	120	283	306	132	426	299	–	369	344
glabra_04	120	283	306	132	426	299	–	369	344
glabra_05	120	283	306	132	426	299	–	369	344
glabra_L186	114	283	304	132	426	297	115	371	344
glabra_L406	114	283	304	132	426	297	115	371	344
glabra_L414	114	283	306	132	426	299	115	371	344
glabra_S388	114	283	306	132	426	299	115	371	344
implexa_L01-01	135	281	323	138	434	316	106	361	350
implexa_L06-05	112	263	323	136	434	316	103	361	350
implexa_L10-03	106	279	323	128	437	316	100	365	346
implexa_L11-15	94	279	323	136	435	316	103	361	352
implexa_L16-15	112	281	325	138	434	318	115	361	352
implexa_S168	112	279	323	138	434	316	115	361	350
implexa_S22	94	279	323	136	436	316	118	361	352
implexa_S36	94	279	325	136	434	318	103	361	346
implexa_S39	–	–	323	138	434	316	–	361	350
implexa_S67	94	279	325	136	434	318	103	361	346
inactiva_L206	114	277	317	137	434	311	100	365	350
inactiva_L323b	114	281	316	132	434	310	131	365	350
inactiva_L347	114	277	317	132	434	310	124	365	350
inactiva_L358	109	281	317	132	436	310	106	365	350
inactiva_S239a	109	277	314	132	434	308	100	365	350
inactiva_S384	114	277	316	137	434	310	100	365	350
inactiva_S392	120	281	316	137	434	310	100	365	350
kockiana_L394	94	279	317	136	472	310	109	365	344
kockiana_L396	94	279	317	136	472	310	109	365	344
kuemmerleana_L04-03	129	279	325	138	434	318	103	361	352
kuemmerleana_L09-04	112	281	323	128	437	316	100	365	346
kuemmerleana_L09-07	112	281	323	128	437	316	100	365	346
kuemmerleana_L16-17	112	281	323	138	434	316	106	361	352
kuemmerleana_L244	117	279	323	138	434	316	115	361	350
kuemmerleana_L274	94	279	323	136	434	316	103	361	352
kuemmerleana_L275	94	279	323	136	434	316	103	361	352
kuemmerleana_S128	100	279	323	136	434	316	100	361	354
kuemmerleana_S160	117	279	323	138	434	316	103	361	350

Appendix 3 (cont.)

Sample	Bi01	Bi03	Bi04	Bi05	Bi10	Bi11	Bi12	Bi14	Bi19
pikei_02	117	277	317	137	434	310	100	365	344
pikei_04	117	277	317	137	434	310	100	365	344
pikei_05	117	277	317	137	434	310	100	365	344
pikei_07	117	281	317	137	434	311	109	–	344
pikei_09	114	281	317	132	–	310	100	–	344
pikei_10	117	277	317	137	434	311	100	365	344
pikei_11	114	277	317	137	434	310	100	365	344
pikei_12	114	277	–	137	434	–	100	–	344
pikei_13	–	277	317	137	434	310	118	365	344
pikei_14	117	277	317	137	434	310	127	365	344
pikei_15	114	281	317	137	436	310	109	–	344
pikei_a	114	–	323	132	437	316	100	–	346
pikei_b	117	277	317	137	434	311	100	365	344
pikei_c	108	–	–	137	–	314	100	326	344
pikei_d	117	277	–	137	437	310	100	–	344
pikei_L197	114	277	316	132	434	310	109	365	344
pikei_L210	109	277	316	132	434	310	100	365	344
pikei_L241	126	277	316	137	434	310	109	–	352
pikei_L374	114	277	316	137	434	310	106	365	344
pikei_L376	132	277	316	137	434	310	127	365	352
pikei_L377	109	277	316	137	434	310	103	365	344
pikei_S221	109	277	316	132	436	310	106	365	352
pikei_S362	114	281	317	137	434	311	100	365	344
pikei_S368	112	281	316	132	436	310	109	365	344
pikei_S382	114	281	317	137	434	311	100	365	344
pikei_S383a	114	281	317	132	436	311	100	365	344
pikei_S390	114	277	316	137	434	310	100	365	344
pikei_S394	126	277	316	137	434	310	100	365	352
pseudofuscscens_S222	–	277	316	132	–	310	100	365	–
pseudofuscscens_S232	114	277	317	137	436	310	100	365	350
pseudofuscscens_S370	117	277	316	132	434	310	100	365	350
pseudofuscscens_S371	117	281	316	132	434	310	100	365	350
pseudofuscscens_S377	–	277	–	132	434	311	100	365	–
pseudofuscscens_S386	112	277	317	132	438	311	100	365	350
pseudofuscscens_S387	117	277	316	132	434	310	127	365	350
sp_L395	94	273	317	136	460	310	109	365	344
sp_S392	97	283	317	136	472	310	118	365	344
vrangiana_L02-20	112	279	323	138	434	316	106	361	352
vrangiana_L03-07	94	279	325	136	434	318	115	365	346
vrangiana_L05-17	117	281	323	138	434	316	121	361	350
vrangiana_L07-03	94	281	323	138	434	316	118	361	352
vrangiana_L07-19	123	279	323	138	434	316	103	361	350
vrangiana_L08-19	94	281	323	136	436	316	103	361	352
vrangiana_L08-20	94	279	323	138	434	316	121	361	352
vrangiana_L10-13	123	283	323	128	437	316	100	365	346
vrangiana_L12-11	94	279	323	138	434	316	144	361	352
vrangiana_L13-12	94	279	323	138	434	316	103	361	352
vrangiana_L272	112	279	323	136	434	316	–	361	350
vrangiana_L273	94	279	323	138	436	316	103	361	350
vrangiana_L300	94	281	323	136	434	316	115	361	350
vrangiana_L307	123	279	325	138	434	318	103	361	352
vrangiana_S10	123	279	323	136	434	316	124	361	352
vrangiana_S164	94	279	323	136	434	316	127	361	350
vrangiana_S166	117	279	323	138	434	316	144	365	352
vrangiana_S196a	94	281	323	138	434	316	118	361	350
vrangiana_S341	–	279	323	–	434	316	–	361	350
vrangiana_S385	94	279	323	138	434	316	103	361	350
vrangiana_S42	117	279	323	138	434	316	131	361	352
vrangiana_S45	112	279	323	136	434	316	100	361	350
vrangiana_S57	94	279	323	138	434	316	115	361	352
vrangiana_S59	94	279	323	138	434	316	115	361	352
vrangiana_S6	123	279	323	138	434	316	103	361	350
vrangiana_S62	112	279	323	138	434	316	115	361	352
vrangiana_S72	94	279	323	136	436	316	103	361	352



Appendix 4 Haplotype network in *Bryoria* sect. *Implexae* of a concatenated matrix containing ITS, IGS and *GAPDH* sequences. The analysis coded gaps as missing data and used a 95 % connection limit. Numbers represent the specimens shown in Table 1 and colours depict the STRUCTURE microsatellites genepool (Fig. 2). Connecting line length do not depict the genetic distance. Each line represents a single mutation connected by black small circles. Circle size is related with the number of analysed specimens. — * = WDb (Wide Distributed brown cluster) specimens.



Appendix 5 Distribution of *Bryoria* sect. *Implexae* specimens examined. Two samples of geographical interest, not analysed in this study, have been added: *Bryoria kockiana* (Canada, British Columbia, 1982, *Goward 82-1040*, UBC – paratype; cf. Velmala et al. 2014) and *Bryoria fuscescens* (Tanzania, Kilimanjaro, 2016, *Boluda & Kitara*, MAF-Lich. 20750). — Basemap source: U.S. National Park Service (NPS) Natural Earth physical map.